Article

Current Biology

Stem cell-specific ecdysone signaling regulates the development of dorsal fan-shaped body neurons and sleep homeostasis

Graphical abstract

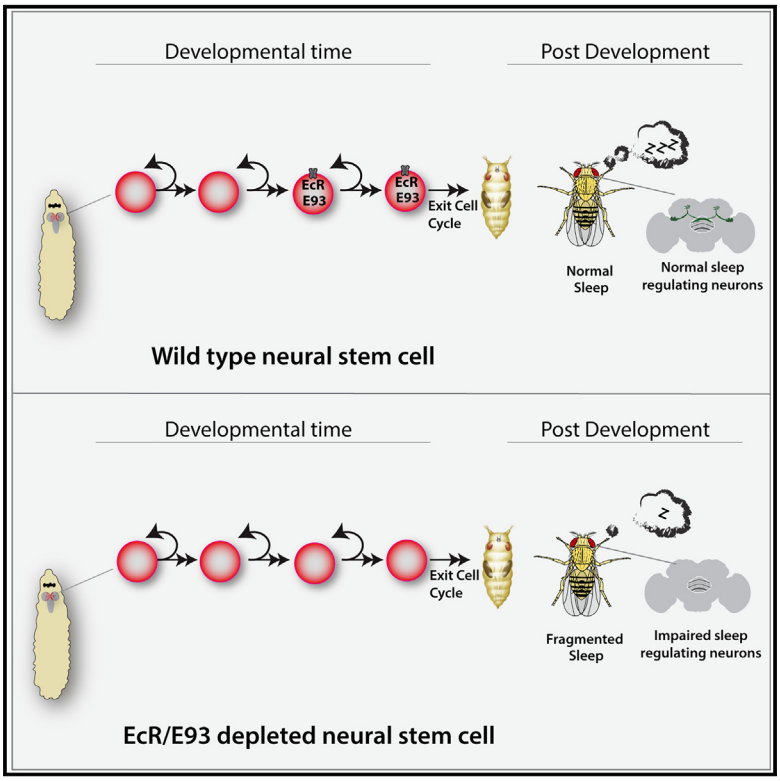

Highlights

- Sleep-regulating 23E10 dFB neurons originate from late larval type II NSCs
- DL1 and DM1 type II NSCs specifically produce 23E10 dFB neurons
- Ecdysone signaling in type II NSCs is essential for 23E10 dFB neuronal fate
- E93 in type II NSCs regulates 23E10 dFB neuronal fate and sleep homeostasis

Authors

Adil R. Wani, Budhaditya Chowdhury, Jenny Luong, ..., Jesse Isaacman-Beck, Matthew S. Kayser, Mubarak Hussain Syed

Correspondence

kayser@pennmedicine.upenn.edu (M.S.K.), flyguy@unm.edu (M.H.S.)

In brief

Wani et al. identify NSCs that generate sleep-regulating 23E10 dFB neurons. They find that ecdysone signaling and E93 in type II NSCs are essential for proper 23E10 dFB neuronal fate. Disruption of E93 expression in type II NSCs causes sleep abnormalities, suggesting that developmental hormonal signaling is critical for adult sleep behavior.

Wani et al., 2024, Current Biology *34*, 4951–4967
November 4, 2024
https://doi.org/10.1016/j.cub.2024.09.020

CellPress

Current Biology

CellPress
OPEN ACCESS

Article

Stem cell-specific ecdysone signaling regulates the development of dorsal fan-shaped body neurons and sleep homeostasis

Adil R. Wani,[1] Budhaditya Chowdhury,[2] Jenny Luong,[3] Gonzalo Morales Chaya,[1] Krishna Patel,[1] Jesse Isaacman-Beck,[4] Matthew S. Kayser,[3,5,*] and Mubarak Hussain Syed[1,6,7,*]

[1]Neural Diversity Lab, Department of Biology, University of New Mexico, 219 Yale Blvd Ne, Albuquerque, NM 87131, USA
[2]The Advanced Science Research Center, City University of New York, New York, NY 10031, USA
[3]Department of Psychiatry, Perelman School of Medicine at the University of Pennsylvania, Philadelphia, PA 19104, USA
[4]Department of Neurobiology, Stanford University, Stanford, CA 94305, USA
[5]Chronobiology Sleep Institute, Perelman School of Medicine at the University of Pennsylvania, Philadelphia, PA 19104, USA
[6]X (formerly Twitter): @neuroseq
[7]Lead contact
*Correspondence: kayser@pennmedicine.upenn.edu (M.S.K.), flyguy@unm.edu (M.H.S.)
https://doi.org/10.1016/j.cub.2024.09.020

SUMMARY

Complex behaviors arise from neural circuits that assemble from diverse cell types. Sleep is a conserved behavior essential for survival, yet little is known about how the nervous system generates neuron types of a sleep-wake circuit. Here, we focus on the specification of *Drosophila* 23E10-labeled dorsal fan-shaped body (dFB) long-field tangential input neurons that project to the dorsal layers of the fan-shaped body neuropil in the central complex. We use lineage analysis and genetic birth dating to identify two bilateral type II neural stem cells (NSCs) that generate 23E10 dFB neurons. We show that adult 23E10 dFB neurons express ecdysone-induced protein 93 (E93) and that loss of ecdysone signaling or E93 in type II NSCs results in their misspecification. Finally, we show that E93 knockdown in type II NSCs impairs adult sleep behavior. Our results provide insight into how extrinsic hormonal signaling acts on NSCs to generate the neuronal diversity required for adult sleep behavior. These findings suggest that some adult sleep disorders might derive from defects in stem cell-specific temporal neurodevelopmental programs.

INTRODUCTION

Proper brain function relies on generating a diverse array of cell types at the appropriate time and place.[1] All neural (neurons and glia) cell types arise from a pool of progenitors called neural stem cells (NSCs).[1–8] During development, NSCs divide to both self-renew and produce distinct classes of neural subtypes over time. These processes are governed by spatial and temporal programs.[9–13] As NSCs age, they express distinct cohorts of genes; this phenomenon is called temporal patterning, allowing individual NSCs to generate a diverse array of neural progeny over time.[1,3–8] The concept of temporal patterning was first described in the *Drosophila* embryonic NSCs, which produce simple larval lineages.[14] Later, similar principles were also observed in the *Drosophila* larval NSCs that generate lineages of the adult brain,[15–19] as well as mammalian neural progenitors that generate the retina, spinal cord, and cortex.[20–27] Although much is known about the temporal patterning mechanisms of the *Drosophila* NSCs, how these mechanisms guide the development of the adult central complex (CX) lineages remains unclear.

The insect CX is a higher-order brain center regulating complex behaviors such as navigation,[28–40] locomotion,[29,41–46] feeding,[47,48] and sleep.[49–60] It is centrally located in the brain and consists of four major neuropils: the handlebar-shaped protocerebral bridge (PB), the fan-shaped body (FB), the doughnut-shaped ellipsoid body (EB), and a pair of noduli (NO).[29,36,61,62] Two orthogonally arranged neuron types divide the CX neuropil into columns and layers: columnar (small-field) neurons divide the neuropil structure into distinct columns along the anteroposterior axis and tangential (large-field) neurons send projections and provide input from lateral brain neuropil to the CX.[36,61,62] Recent connectome data have identified ~257 unique neural types in the CX that are believed to regulate various behaviors.[36] How this diversity arises during development is not completely understood.

The neural lineages of the CX are generated, in part, by the relatively rare "type II" NSCs.[63–68] The larval type II NSCs occupy distinct brain regions and are organized into dorsomedial (DM) (1–6) and two dorsolateral (DL1 and 2) groups. Although there are only sixteen type II NSCs, they produce more complex and diverse lineages by generating transit-amplifying intermediate neural progenitors (INPs)[69–71] (Figure 1A). Each type II NSC produces around 40–50 INPs,[65] and each INP divides 4–5 times to produce about ten progeny; hence, each type II NSC is thought to generate approximately 400–500 progeny.[63,72] This division pattern of type II NSCs is reminiscent of a division pattern of the primate outer radial glia (oRG) that generate lineages

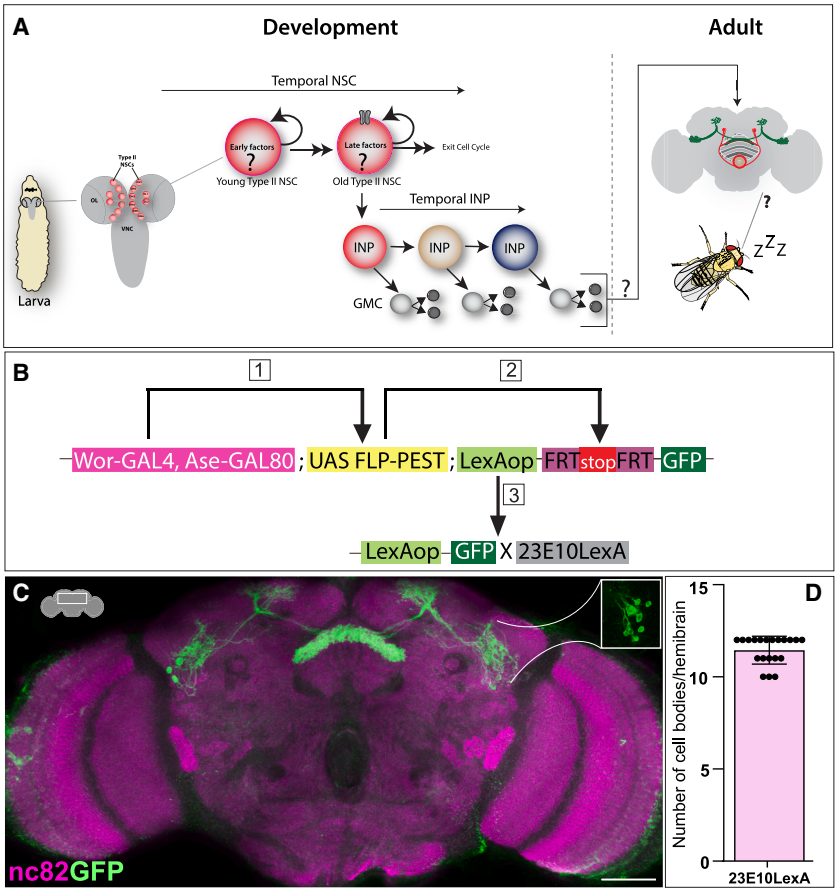

Figure 1. Type II NSCs produce 23E10 dFB neurons

(A) Schematics of larval type II NSCs (8 per lobe: DM1–6 and DL1-2), which divide asymmetrically over 120 h ALH to generate INPs and express early and late temporal factors. The temporally expressed EcR mediates the switch from early to late gene transition. The type II NSC and INP temporal factors are thought to contribute to the formation and diversification of neural lineages of the *Drosophila* central complex. We are investigating the role of ecdysone signaling in the specification and function of 23E10 dFB neurons, which are part of the *Drosophila* sleep-wake circuit.

(B) Schematics showing an intersectional genetic approach for type II NSC lineage analysis utilizing a type-II-NSC-specific flip-out approach. The expression of Asense-GAL80 in type I NSCs ensures that Worniu-GAL4 is only expressed in type II NSCs. Worniu-GAL4 induces type-II-NSC-lineage-specific expression of flippase (FLP) in all type II NSCs, which excises a STOP cassette, activating LexAopGFP expression in a class-specific manner when crossed to a LexA driver. These flip-out events allow 23E10 dFB neurons to be labeled in green if produced from type II NSCs.

(C) The 23E10 dFB neurons are labeled by reporter GFP in a type-II-NSC-specific manner. 23E10 dFB neurons are shown in green (max projection), and nc82 labels neuropil (magenta) (projections showing only FB). The expression of GFP reporter in 23E10 dFB neurons confirms that they are derived from type II NSCs.

(D) Quantification of the number of 23E10 dFB neuron cell bodies per hemibrain flipped by type II NSC filtering. Error bars represent ± SD.

Scale bars represent 40 μm. n = 20 adult hemibrains.

containing INPs and make neurons of the cortex.[73–76] Studying how type II NSCs produce diverse lineages of the CX may provide insights into the mechanisms that regulate neural diversity in mammals. Additionally, the NSCs that generate most columnar neurons of the CX are conserved in all insects studied to date.[77–84] Therefore, understanding how CX neurons are produced in *Drosophila* will likely reveal conserved developmental mechanisms.

Clonal analysis has revealed unique contributions of each type II NSC to the adult CX neuropil structures.[63,64,68] Among type II NSCs, four (DM1–4) generate columnar neurons, while DL1 primarily generates long-field tangential neurons.[63,64] However, DM4 and DM6 also produce some long-field neurons, reflecting diverse classes of tangential input neurons.[63,64] Additionally, each type II NSCs generates distinct classes of neurons and glia over time.[7,15,17,65,67,72] Temporal clonal analysis has revealed that INPs generate neurons of distinct identities after each division,[7,65,72] suggesting that type II NSCs and INPs employ combinatorial temporal programs to diversify CX cell types.[7,72] How might type II NSCs and INPs generate the temporally distinct program generating neuronal diversity? Recent studies have shown that larval type II NSCs express a set of transcription factors (TFs) and RNA-binding proteins (RBPs) with precise temporal specificity.[15,17] Young type II NSCs express early factors such as Castor, Sevenup, Chinmo, insulin growth factor (IGF)-II mRNA-binding protein (Imp), and Lin-28; later, as they age, they switch to expressing ecdysone receptor (EcR), broad, ecdysone-induced protein 93 (E93), and Syncrip.[15,17,19] Interestingly, the expression of EcR around ∼55 h after larval hatching (ALH) mediates early to late gene transition via NSC extrinsic ecdysone signaling.[15] Thus, unlike embryonic NSCs and larval optic lobe NSCs, generating complex adult lineages requires coordination of both stem cell-intrinsic and -extrinsic programs.[7,15] However, whether these temporally expressed genes and ecdysone play any role in the fate specification and function of the adult CX neurons is currently unknown. Furthermore, whether these temporal molecular cues regulate adult behaviors remains unexplored.

Sleep is an evolutionarily conserved behavior essential for numerous physiological functions.[60,85,86] The *Drosophila* CX has repeatedly been implicated as an axis for sleep-wake regulation.[50–53,57,58,87–90] One brain area that has received particular attention is the FB of the CX, where 23E10-GAL4-labeled sleep-regulating dFB neurons (subsequently called 23E10 dFB neurons) innervate and regulate sleep homeostasis. These neurons are classified as long-field tangential input neurons and there are ∼12 on each side of the brain.[51] Activation of 23E10 dFB neurons induces sleep,[50,51] and these neurons are more excitable following sleep deprivation.[52] Despite extensive evidence for a function in sleep regulation, controversy has emerged regarding the specific role of 23E10-GAL4-defined cells. The 23E10-GAL4 driver line labels cells in the ventral nerve cord (VNC) in addition

to those in the brain dFB, and these VNC cells appear sufficient to regulate sleep.[91,92] However, more recent work using intersectional genetic approaches demonstrates that 23E10+ dFB neurons of the brain also include bona fide sleep-regulatory cells and suggests that these cells play a specialized role in encoding sleep pressure.[93–95] Little is known regarding the developmental origin of these 23E10 dFB sleep neurons. More broadly, although linking sleep behavior to a unique NSC population is challenging in vertebrates, understanding the development of the sleep-wake circuit is crucial, as many neurodevelopmental disorders arise due to impairments in neurogenesis, circuit formation, and comorbid sleep defects with more fragmented sleep architecture.[96–101]

In this study, we focus on the lineage analysis and development of the 23E10 dFB neurons. Using sophisticated genetics and lineage analysis, we have identified the NSCs that generate the 23E10 dFB neurons involved in regulating sleep behavior. Specifically, we show that most 23E10 dFB neurons originate from the DL1 type II NSC, while 1–2 dFBs are born from the DM1 NSC. We also demonstrate that 23E10 dFB neurons are generated between 48 and 76 h ALH and that steroid-hormone-signaling-induced E93 specifies these neurons. Finally, we show that NSC-specific E93 is essential for normal sleep homeostasis. Our findings reveal the developmental origin and birth timing of 23E10 dFB neurons and establish the importance of steroid hormonal signaling and E93 in governing the proper development and function of 23E10 dFB neurons.

RESULTS

23E10 dFB neurons are born from type II NSCs

Most neurons and glia derived from type II NSCs populate the CX of the adult *Drosophila* brain, including local and long-field tangential input neurons.[63,64,68] To determine whether 23E10 dFB neurons originate from type II NSCs, we used intersectional genetics. We employed a type-II-NSC-specific flippase (FLP) enzyme to permanently remove the stop cassette from LexAop-FRT-stop-FRT-mCD8GFP and a cell-class marker 23E10-LexA to label 23E10 dFB neurons in the adult brain. In this intersectional approach, if the neurons of our interest are derived from type II NSCs, they will be labeled in green in the adult brain. We expressed FLP in all type II NSCs using the Wor-GAL4, Ase-GAL80 driver, which made the LexAop-FRT-stop-FRT-mCD8GFP reporter functional only in type II NSCs (Figure 1B). As a result, we observed all 12 bilateral 23E10 dFB neurons were labeled green (Figures 1C and 1D), confirming that all 23E10 dFB neurons are derived from type II NSCs. We observed that the 23E10-LexA driver labels neurons other than dFBs outside of the CX region; however, upon type II NSC filtering, only dFB neurons that project to the CX were labeled with GFP (Figure 1C). Thus, we have identified that 23E10 dFB neurons whose cell bodies are in the protocerebral posterior lateral (PPL) region and project to the FB originate from type II NSCs.

Two distinct type II NSCs generate 23E10 dFB neurons

Previous studies have provided a reference framework of the developmental organization of the *Drosophila* brain by assigning unique clone morphologies to each NSC in the larval central brain.[63,64,68] The DM1–4 type II NSCs generate most local columnar neurons, while DL1 generates the majority of long-field tangential input neurons, with minor contributions from DM4 and DM6.[63,64,102] To determine which type II NSCs generate 23E10 dFB neurons, we used a heat-shock-based lineage filtering method called cell-class-lineage analysis (CLIn).[103] This method classifies type II NSC lineages by assigning cells to specific categories based on their clone morphology and connectivity patterns.[103] Using CLIn, one can generate individual type II NSC clones by giving a temporal heat shock during development. In a successful flip-out event, the entire lineage of the type II NSCs is labeled by mCherry (reporter A). At the same time, the specific neuronal type marked by the GAL4 will be labeled with the GFP (reporter B) (Figures 2A and 2B).

Using CLIn method, we induced a 10- to 12-min heat shock at 0 h ALH and analyzed individual type II NSC clones labeled with mCherry, pseudo-colored with cyan in the adult brain (see STAR Methods for detailed protocol). We generated single type II NSC clones, then compared these with previously published clonal maps to assign lineages to the 23E10 dFB neurons.[63,64,68] Our findings revealed that most 23E10 dFB neurons (~10) are derived from DL1 (Figure 2C), while ~1–2 neurons are generated by DM1 type II NSCs (Figure 2D). This mixed lineage indicates heterogeneous cell types within the 23E10 dFB cluster. Previous clonal studies may have missed the contribution of DM1 in generating long-field tangential neurons, as these neuron types were not assigned to DM1 lineages (see discussion).

23E10 dFB neurons are generated by late type II NSCs

Type II NSCs express different gene classes during the early and late phases of their lineage, which are thought to regulate the identity of the neurons born during these periods.[6,7,15,17,104] To determine whether 23E10 dFB neurons are born from early or late type II NSCs, we performed genetic birthdating using CLIn method. We applied heat shocks at different times during larval development. Briefly, we crossed 23E10-GAL4, which labels 23E10 dFB neurons, to the CLIn fly (for genotype, see STAR table) and applied heat shock to the progeny at three major development time points: 0, 48, and 76 h ALH (Figure 2E). There are two phases of neurogenesis, embryonic and larval.[1,6,7,105–107] While most embryonic-born neurons die during metamorphosis,[108–113] a small population survives, undergoes metamorphosis,[112,114,115] and contributes to the adult brain.[115–118] The neurons and glia generated in the larval phase of neurogenesis predominantly contribute to adult brain circuits.[63,64,68,119] When we performed 0 h ALH heat shock, we observed all the 23E10 dFB neurons labeled in the adult brain, confirming that all 23E10 dFB neurons are produced post embryonically (Figure 2F). Next, we wanted to narrow down their birth time precisely to the time they are derived from type II NSCs and performed heat shock at 48 and 76 h ALH. Heat shock at 48 h ALH labeled most 23E10 dFB neurons, while heat shock at 76 h ALH did not label any neurons, confirming that 23E10 dFB neurons are born between 48 and 76 h ALH (Figures 2F and 2G). Taken together, we conclude that sleep-regulating 23E10 dFB neurons are born from late DL1 and DM1 type II NSCs—at the time of EcR-mediated temporal gene expression.[15]

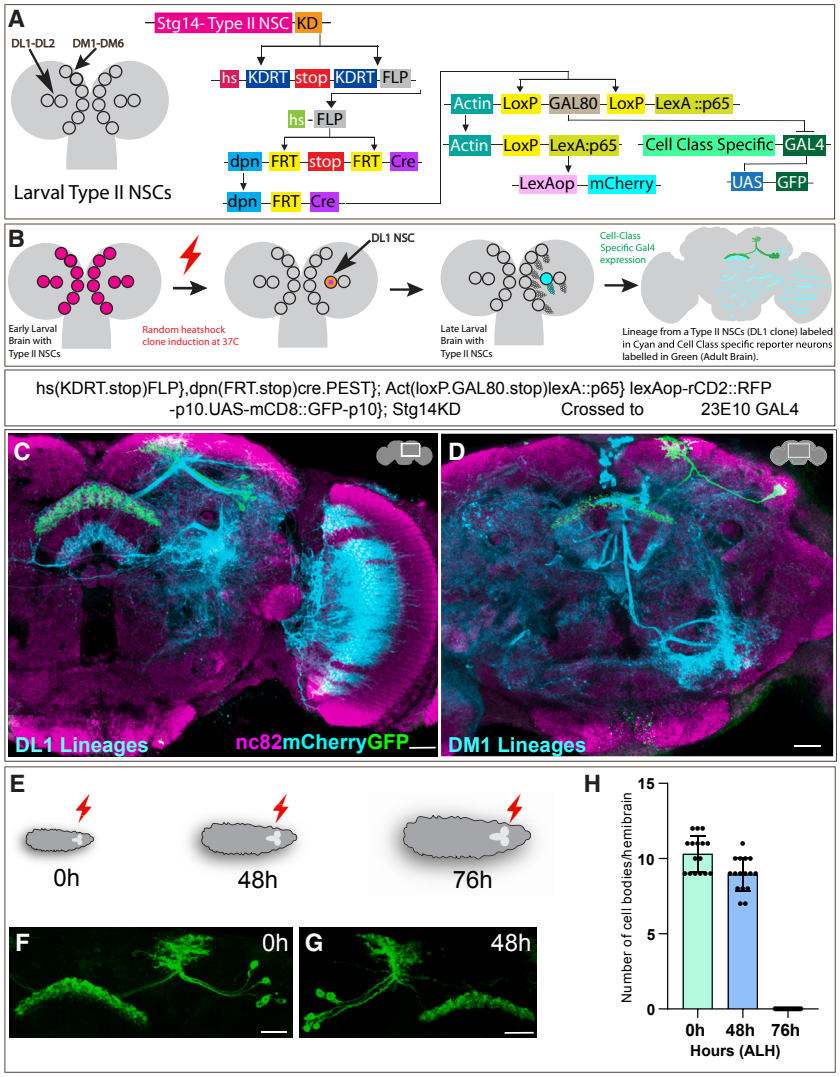

Figure 2. 23E10 dFB neurons are generated by late DL1 and DM1 type II NSCs

(A) The schematic of CLIn intersectional genetics illustrates the genetic components enabling lineage analysis and genetic birth dating of type II NSC lineages. The CLIn flies use a type-II-NSC-specific promotor, stg14 (magenta), to express KD recombinase specifically in type II NSCs. KD recombinase removes a stop sequence, bringing FLP recombinase (gray) in frame with a heat shock promotor, but only in type II NSCs. Upon heat shock, FLP is stochastically expressed, removing another stop sequence and activating Cre recombinase (purple), specifically in type II NSCs. The active Cre recombinase removes GAL80 and makes LexA::p65 active, thus enabling the lineage-specific expression of reporter mCherry (cyan) and the expression of mCD8GFP in a class-specific manner possible when crossed to GAL4. (Adopted from Ren et al.)[103]

(B) The schematic shows how CLIn allows lineage analysis of type II NSCs. The stochastic heat-shock-mediated FLP event in a DL1 type II NSC labels all neurons and glia with mCherry (cyan) born from this NSC and, when crossed to a cell-class-specific GAL4, co-labels the neurons with GFP.

(C) Composite confocal image of a single DL1 NSC clone induced at 0 h ALH labels most 23E10 dFB neurons (green). All lineages from DL1 NSC are labeled in cyan (mCherry), and the neuropil of the adult fly brain is stained with nc82 (magenta).

(D) Confocal image of single DM1 NSC clone induced at 0 h ALH labels 1–2 23E10 dFB neurons. The DM1 lineages are labeled in cyan (mCherry) and the neuropil of the adult fly brain is stained with nc82 (magenta).

(E) The schematic illustrates heat shock administered at various time points during larval development. The red lightning bolt symbol indicates heat shock given at three specific time points: 0, 48, and 76 h after larval hatching (ALH).

(F–H) Clones induced at 0 and 48 h ALH label the 23E10 dFB neurons (F and G), whereas clones induced at 76 h ALH do not label any 23E10 dFB neurons.

(H) Quantification of 23E10 dFB neuron cell bodies labeled per hemibrain when clones are induced at 0, 48, and 76 h ALH. Error bars represent ± SD. Scale bars represent 20 μm, n = 16 adult hemibrains for each time point.

Ecdysone signaling in type II NSCs is required for 23E10 dFB neuronal fate

The insect growth hormone ecdysone regulates various stages of nervous system development, including neurogenesis, refining neural connections through pruning and regulating programmed cell death.[111,112,114,120–123] In *Drosophila*, ecdysone is present in varying concentrations throughout development[112,121,124]; however, type II NSCs express EcR temporally, which transduces the extrinsic hormonal signal into the cell to regulate temporal gene expression.[15] To investigate the role of type-II-NSC-specific EcR in 23E10 dFB fate specification, we generated an EcR-FLPStop2.0 transgenic fly. FLPStop2.0 is a modified and efficient version of the conditional loss-of-function strategy using the FLPStop technique[125] (Figure 3A), with an added repeated ribozyme motif known to disrupt expression[126] (Figure 3A; STAR Methods). This method was needed due to the failure of EcR-RNAi to knock down EcR levels in type II NSCs. In the FLPStop method, tissue-specific FLP recombinase expression inverts the cassette, which results in a premature stop; as a result, a conditional loss-of-function allele is generated (Figure 3A). Upon this inversion, the fluorescent tag upstream-activating sequence (UAS)-tdTomato becomes functional and labels mutant cells in red color[125] (Figure 3A). To check whether EcR-FLPStop2.0 abolishes the EcR function, we expressed FLP in type II NSCs by crossing Pointed-GAL4 to UAS-FLP in the EcR-FLPStop2.0 background. We also added lineage-tracing cassette Act-FRT-stop-FRT-GAL4 to trace mutant lineages to the adult brain (see STAR table genotype). In the progeny with the genotype UAS-FLP, Act-FRT-stop-FRT-GAL4; UAS-EcR-FLPStop2.0/Pointed-GAL4, all the EcR loss-of-function progeny were labeled in red, and we observed a significant reduction of EcR and E93 protein in type II NSCs and their progeny (Figures S1A–S1B′), confirming that EcR-FLPStop2.0 severely reduces EcR function. In the EcR-FLPStop2.0 background, we used 23E10-LexA, LexAop-mCD8GFP to label dFB neurons in green. In the progeny with the genotype UAS-FLP,

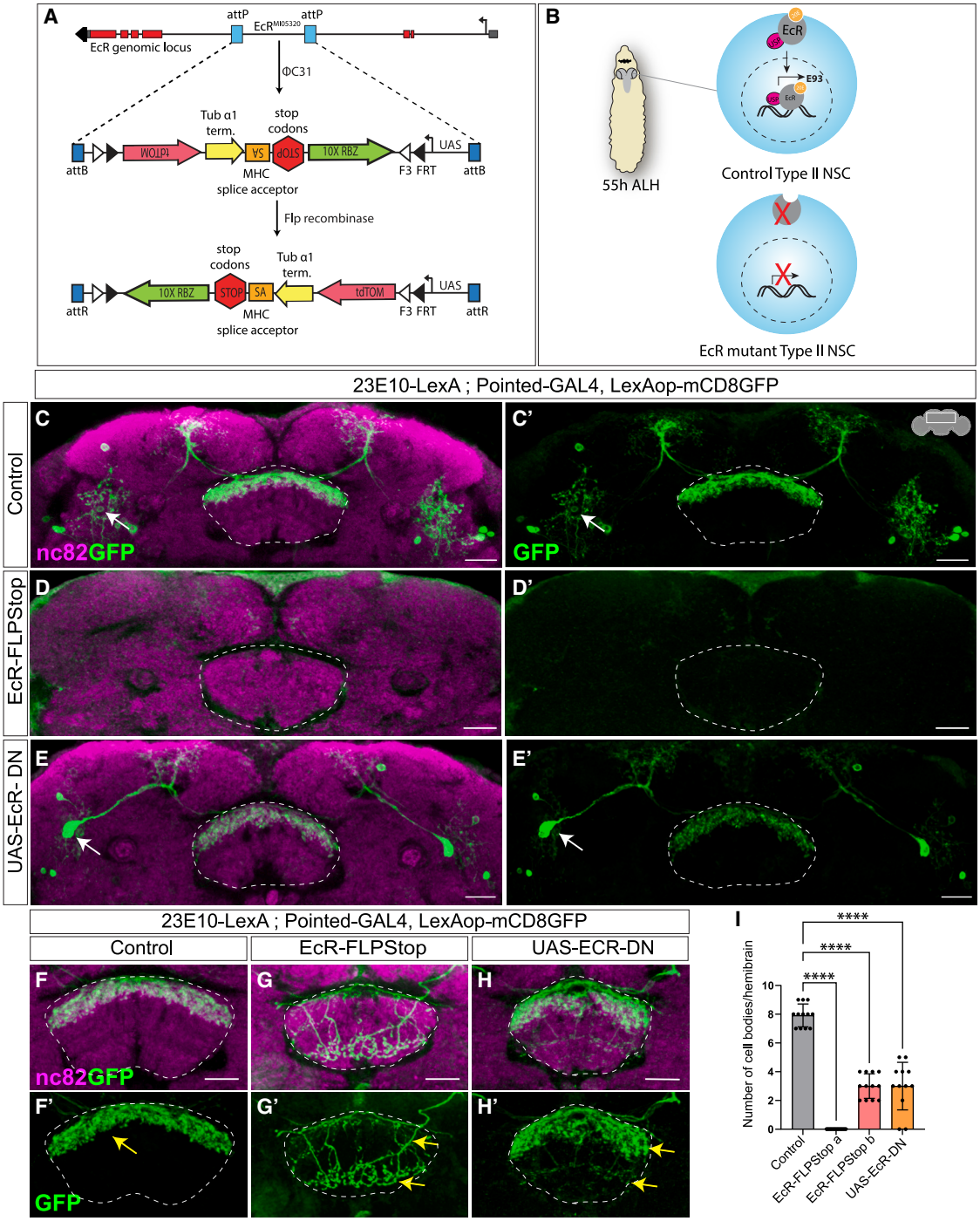

Figure 3. Ecdysone signaling regulates 23E10 dFB neuron specification

(A) A schematic illustrating EcR-FlpStop2.0 conditional knockout strategy. In this strategy, the expression of FLP recombinase in type II NSCs flips the tdTomato sequence into the correct frame with a UAS promoter, allowing it to label mutant cells specifically under the control of type-II-specific GAL4 in red color. Additionally, the FLP event also inverts the STOP sequence—transcription-based disruption (Tubα1terminator and 10× ribozyme sequence) and translation disruption (major histocompatibility complex [MHC] splice acceptor paired with STOP codons)—to generate a premature stop, disrupting EcR expression and function.

(B) A schematic depicting a normal type II NSC expressing EcR at 55 h ALH, which results in the activation of EcR-induced downstream genes. When EcR function is lost, the expression of downstream genes is disrupted.

(C and C′) Shows a control brain with dFB neurons labeled by 23E10-LexA driving GFP expression, highlighting their projection pattern in the FB. The nc82 (magenta) labels the neuropil in the adult brain in all subsequent figures.

(legend continued on next page)

Act-FRT-stop-FRT-GAL4; UAS-EcR-FLPStop2.0, 23E10-LexA; Pointed-GAL4, LexAop-mCD8GFP, we were able to simultaneously create EcR loss of function in type II NSCs and label 23E10 dFB neurons in the adult brain. We examined whether loss of EcR in type II NSCs leads to defects in the specification, morphology, or connectivity of the 23E10 dFB neurons. There are ~12 23E10 dFB neurons on each side of the brain, with cell bodies located in the PPL region. These neurons send the axonal projections to layer 6 of the dorsal FB, where they are thought to connect with the helicon cells to regulate sleep homeostasis.[53] In most experimental flies, depletion of EcR in type II NSCs resulted in the loss of 23E10 dFB neurons in the adult brain (Figures 3C–3D′ and 3I), indicating that ecdysone signaling in type II NSCs is necessary for the formation of 23E10 dFB neurons.

To further investigate whether the steroid hormone ecdysone regulates 23E10 dFB fate and connectivity, we use EcR dominant negative (DN)[127] to block ecdysone signaling. We specifically blocked ecdysone signaling in larval type II NSCs by expressing EcR-DN with Pointed-GAL4 and assayed the fate of 23E10 dFB neurons in the adult brain. We found that blocking ecdysone signaling in type II NSCs affects 23E10 dFB fate, reducing 23E10 dFB neuron numbers, similar to the EcR loss of function (Figures 3E, 3E′, and 3I). However, in EcR loss-of-function animals, we found some animals with a less-penetrant phenotype, where a few neurons were present (Figures 3F–3G′). Interestingly, the connectivity of the surviving neurons was severely disrupted (Figures 3G and 3G′). Compared with the control brains (Figures 3F and 3F′), where 23E10 dFB neurons send their axonal projections to layer 6 of the dorsal region of the FB, in EcR loss of function (Figures 3G and 3G′), surviving neurons ectopically project to the ventral layers of the FB. A similar mistargeting phenotype was observed in the surviving 23E10 dFB neurons in EcR DN experimental animals (Figures 3H and 3H′), indicating multiple roles of EcR and ecdysone signaling in specifying 23E10 dFB neurons that are part of the sleep-wake circuit (see discussion). Taken together, our findings suggest that type-II-NSC-specific ecdysone signaling is essential for the proper formation and identity of the 23E10 dFB neurons (Figure 3I). Upon misexpression of EcR in type II NSCs throughout development, we did not observe any increase in the 23E10 dFB neuron numbers (Figures S1C–S1E), indicating that EcR alone is not sufficient for generating 23E10 dFB neuron types. Taken together, our studies link an extrinsic hormonal signal to the NSC-intrinsic gene programs via temporal expression of EcR in late NSCs to generate 23E10 dFB neurons.

Using nc82 staining, we found that EcR loss of function in type II NSCs specifically affects the EB neuropil development. Compared with the control (Figures S1F and S1G), there was a severe defect in the EB, which did not fuse in experimental flies (Figures S1F′ and S1G′). To our knowledge, these findings are the first to relate the extrinsic ecdysone signal to stem cell-intrinsic gene programs to specify 23E10 dFB neuronal fate and CX development.

Ecdysone induces E93, which regulates 23E10 dFB fate

Next, we wanted to understand how type-II-NSC-specific ecdysone signaling regulates 23E10 dFB neuronal specification. Our previous work identified ecdysone signaling as the primary regulator of early to late gene transitions in type II NSCs.[15] Around ~55 ALH, temporal expression of EcR in type II NSCs activates late genes (Figure 1A), including the ecdysone-induced gene, E93 (Figure 3B). Interestingly, all 23E10 dFB neurons express nuclear E93 (Figures 4A–4A″), suggesting that EcR may specify 23E10 dFB neuronal fate via E93. To test this hypothesis, we knocked down E93 in all type II NSCs during development using Pointed-GAL4 and analyzed the adult dFB neurons labeled with 23E10-LexA, LexAop-mCD8GFP. The efficiency and specificity of E93 knockdown (UAS-E93RNAi) were confirmed by staining larval type II NSCs for E93 expression (Figures S2A and S2B). For the control experiments, we crossed Pointed-GAL4 to an empty RNAi, UAS-KKRNAi, which has the same genetic background as UAS-E93RNAi (see STAR Methods). Compared with the control (Figures 4B and 4B′), E93 knockdown in type II NSCs resulted in the absence of all 23E10 dFB neurons (Figures 4C and 4C′), quantified in (Figure 4H). This indicates that E93 expression in type II NSCs is essential for the specification of 23E10 dFB neurons. In the experimental flies, we noticed that 2–3 cell bodies were always present; however, we observed them in the controls as well, and these neurons are not part of the 23E10 dFB cluster because they do not send projections to the dFB. Taken together, we conclude that the late temporal expression of E93, activated by EcR, regulates the formation of adult 23E10 dFB neurons. To confirm that the observed phenotype is E93 specific, we repeated the experiments using E93 RNAi without dicer and another independent E93 RNAi line (Figures S2C–S2D′ and S2F; see STAR Methods). Both conditions showed similar phenotypes, with the E93 RNAi with dicer producing a more severe phenotype (Figures 4C, 4C′, S2C–S2D′, and S2F). Unlike EcR loss of function, E93 knockdown did not affect the adult CX neuropil morphology (Figures S3A–S33B″), suggesting that E93 specifically regulates 23E10 dFB neuronal fate without influencing the broader CX neuropil development.

Next, we wanted to test whether E93 is sufficient to specify 23E10 dFB neurons. We used Pointed-GAL4, UAS-E93 to express E93 in type II NSCs throughout larval development and 23E10-LexA, LexAop-mCD8GFP to label dFB neurons. Compared with the control (Figures 4B and 4B′), we did not observe any extra 23E10 dFB neurons in experimental animals

(D and D′) Upon EcR loss of function in type II NSCs, 23E10 dFB neurons are not specified
(E and E′) Blocking ecdysone signaling in type II NSCs using EcR-DN results in significant loss of 23E10 dFB neurons.
(F–H′) In control brains, the 23E10 dFB neurons project to layer 6 of the FB (F and F′). In animals with EcR loss of function (G and G′), or expressing EcR-DN (H and H′), the surviving dFB neurons misproject to the ventral FB layers indicated by yellow arrows.
(I) One-way ANOVA test (followed by Dunnett's multiple comparison test) quantification of 23E10 dFB neuron cell bodies. Error bars represent ± SD. Asterisks indicate the level of statistical significance: *$p < 0.05$, **$p < 0.01$, ***$p < 0.001$, **** $p < 0.0001$; NS, non-significant.
Cell bodies are indicated by white arrows. The dashed line outlines the FB.
Scale bars represent 20 μm, $n = 12$ adult hemibrains. See also Figure S1.

CellPress
OPEN ACCESS

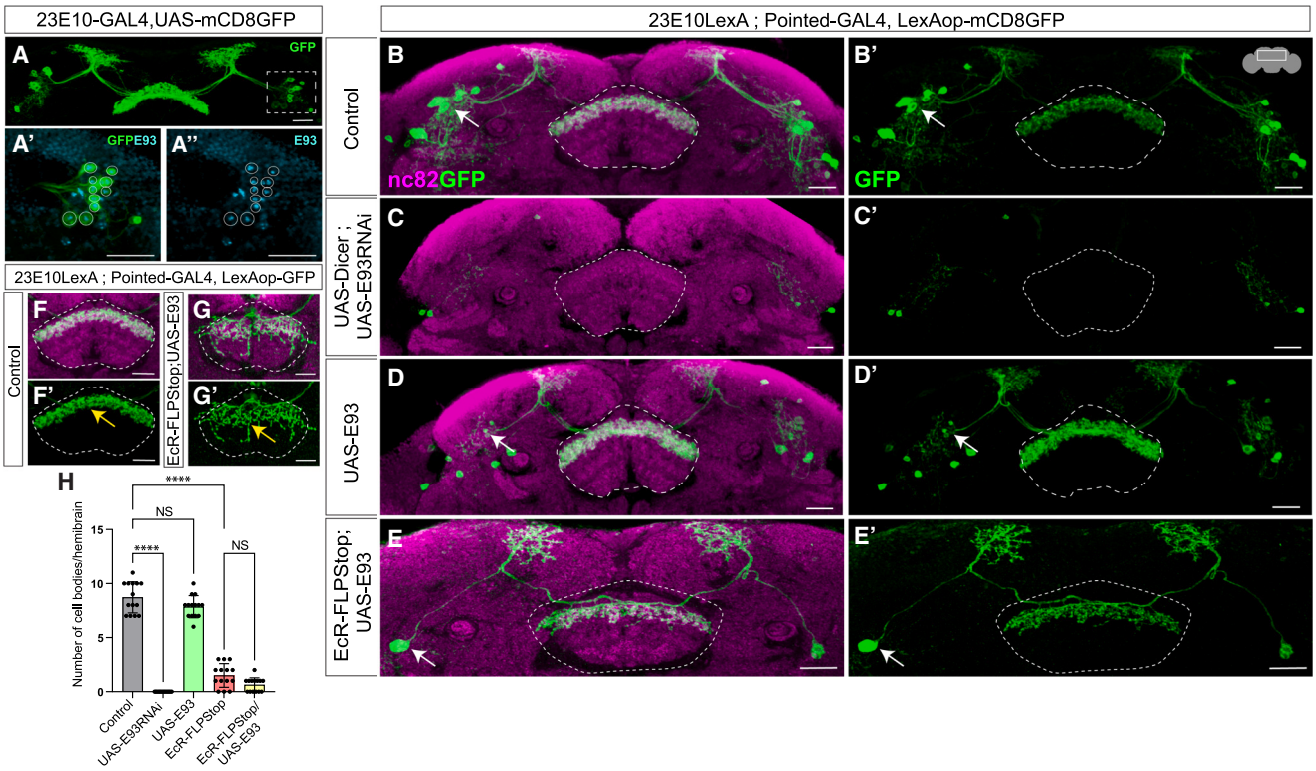

Figure 4. Ecdysone-induced gene E93 is necessary for 23E10 dFB fate

(A) 23E10 dFB neurons, labeled in green (A), express E93 in cyan (A′ and A″).

(B) Control dFB neurons labeled by 23E10-LexA project to the dorsal FB.

(C) E93 knockdown in type II NSCs using Pointed-GAL4 results in the complete loss of 23E10 dFB neurons (C and C′).

(D) E93 overexpression in type II NSCs using Pointed-GAL4 does not alter the number or morphology of 23E10 dFB neurons (D and D′).

(E) Expression of E93 under Pointed-GAL4 fails to rescue 23E10 dFB neurons in EcR loss-of-function background (E and E′).

(F–G′) Compared with control brains (F and F′), the experimental brains with UAS-E93 expressed in EcR loss-of-function background show defects in axonal targeting (G and G′). The axonal projections of 23E10 dFB neurons ectopically innervate ventral layers of FB, as indicated by yellow arrows.

(H) Quantification of 23E10 dFB neuron cell bodies per hemibrain using one-way ANOVA test followed by Šidák's multiple comparison test. Error bars represent mean ± SD; asterisks indicate the level of statistical significance: $^{*}p < 0.05$, $^{**}p < 0.01$, $^{***}p < 0.001$, $^{****}p < 0.0001$; NS, non-significant.

Cell bodies are indicated by white arrows. The dashed line outlines the FB.

Scale bars represent 20 μm, $n = 14$ adult hemibrains for each genotype. See also Figures S2 and S3.

(Figures 4D and 4D′), quantified in (Figure 4H), indicating that E93 is not sufficient to generate the 23E10 dFB neuronal fate and rather a combination of factors might be involved. Upon misexpression of E93 in type II NSCs, the overall CX neuropil morphology was not impaired (Figures S3C–S3C″).

To determine whether EcR acts through E93 to specify 23E10 dFB neurons, we performed a rescue experiment by expressing UAS-E93 in the EcR-FLPStop background. We also added lineage-tracing cassette Act-FRT-stop-FRT-GAL4 to track mutant lineages to the adult brain. We made a fly line with genotype UAS FLP, Act-FRT-stop-FRT-GAL4; EcR-FLPStop2.0: UAS-E93 and crossed it to 23E10-LexA; Pointed-GAL4, LexAop-mCD8GFP. This experimental setup allowed for the loss of endogenous EcR and its downstream targets, including E93, while simultaneously expressing exogenous E93 in EcR-depleted type II NSCs. Using this approach, we found that expression of E93 alone in the type II NSCs did not rescue the loss of 23E10 dFB neurons (Figures 4E, 4E′, and 4H), producing a phenotype identical to the EcR loss of function in type II NSCs (Figures 3C–3D′ and 3I). This indicates that both EcR and E93 are necessary for specifying 23E10 dFB neurons. The rescue experiment also resulted in the mistargeting of the surviving neurons, similar to the EcR loss-of-function phenotype (Figures 4F–4G′). Furthermore, overexpression of E93 in an EcR loss-of-function background caused malformation of the FB, EB, and PB (Figures S3D–S3D″), suggesting that precise levels and timing of E93 expression are crucial for normal CX neuropil development.

Next, to exclude the role of Actin-GAL4 in our rescue experimental setup, we set our rescue experiment without the lineage-tracing cassette Act-FRT-stop-FRT-GAL4. Reintroducing E93 using UAS-E93 in the EcR mutant backgrounds did not rescue the 23E10 dFB neuronal fate phenotype, consistent with the previous rescue experiments that included the lineage-tracing cassette (Figures S2E and S2F). However, the CX neuropil structure remained intact (Figures S3E–S3E″), suggesting that misexpression of E93 in postmitotic neurons could be causing the CX neuropil defects. To determine whether the adult brain malformation was due to our experimental setup or the loss of endogenous EcR and E93, we misexpressed E93 in all type-II-derived lineages using Actin flip-out GAL4 active in type II NSCs.

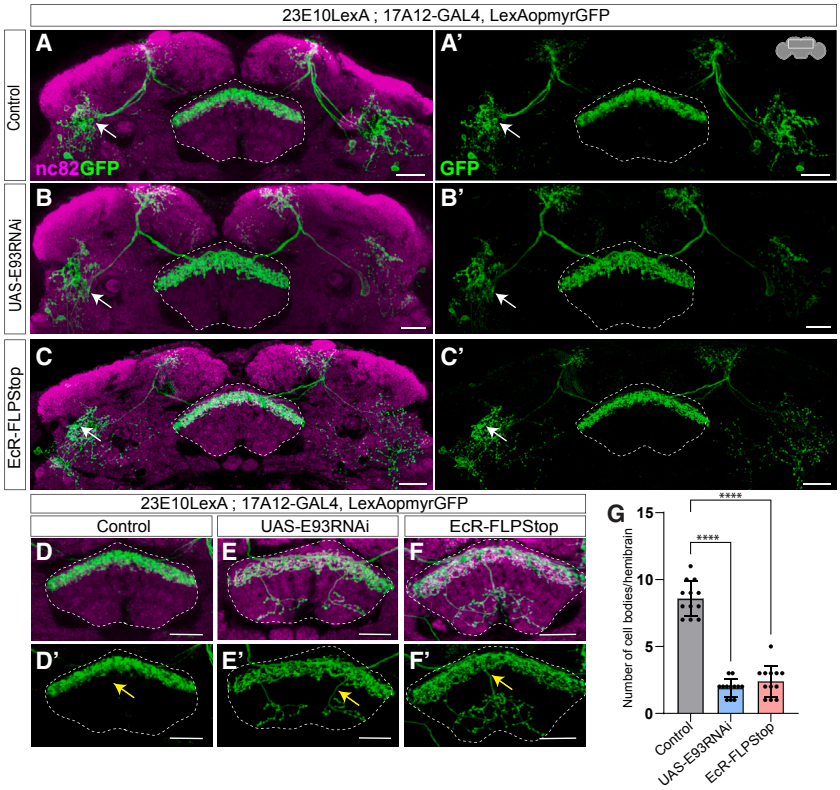

Figure 5. EcR and E93 are required in DL1 type II NSCs to specify 23E10 dFB neurons

(A–G) Control (A), EcR, and E93 loss of function (B and C) show loss of 23E10 dFB neurons, labeled by 23E10-lexA driving GFP expression. In control brains (D and D′), 23E10 dFB neurons exhibit normal axonal projection to the dorsal layers of FB. However, in E93 (E and E′) and EcR (F and F′) loss-of-function conditions, the axonal projections of the 23E10 dFB neurons are impaired and expand into ventral layers of FB, as indicated by yellow arrows.

(G) Quantification of 23E10 dFB neuron cell bodies per hemibrain upon DL1/DL2-specific knockdown of E93 and EcR, analyzed using one-way ANOVA followed by Dunnett's multiple comparison test. Error bars represent mean ± SD. Asterisks indicate the level of statistical significance: $*p < 0.05$, $**p < 0.01$, $***p < 0.001$, $****p < 0.0001$; NS, non-significant.

Cell bodies are indicated by white arrows. The dashed line outlines the FB.

Scale bars represent 20 μm. $n = 12$ adult hemibrains for each genotype.

Overexpression of E93 alone in these lineages resulted in brain neuropil defects similar to those observed in rescue experiments with the lineage-tracing cassette (Figures 4E, 4E′, 4H and S3F–S3F″). Taken together, these findings suggest that both EcR and E93 are required to specify 23E10 dFB neuronal fate (see discussion).

Temporal expression of EcR and E93 in DL1 type II NSCs specifies 23E10 dFB neurons

In our previous experiments, we manipulated the expression of EcR and E93 using Pointed-GAL4, which is expressed in all type II NSCs. To refine our approach and to confirm the specific roles of ecdysone signaling in regulating the 23E10 dFB neuronal fate, we employed 17A12-GAL4, which labels explicitly DL1/DL2 type II NSCs.[128] We used this approach because our lineage-tracing experiments confirmed that most 23E10 dFBs are born from DL1 type II NSCs (Figures 2C and 2D).

Compared with the control (Figures 5A, 5A′, and 5G), the loss of E93 in DL1 type II NSCs using 17A12-GAL4 led to a significant reduction in the number of 23E10 dFB neurons (Figures 5B, 5B′, and 5G). This confirms that DL1-lineage-specific ecdysone signaling is crucial for the specification of 23E10 dFB neurons. Furthermore, we depleted EcR function using EcR-FLPStop (Figure 3A) in DL1 type II NSCs using 17A12-GAL4 and observed a notable decrease in 23E10 dFB neuron number (Figures 5C, 5C′, and 5G) compared with the control (Figures 5A, 5A′, and 5G). These results overall suggest that the expression of EcR and E93 in DL1 NSC is critical for the formation of the most 23E10 dFB neurons. The remaining neurons observed after the loss of EcR and in DL1 type II NSCs might originate from other type II NSCs, such as DM1, as confirmed by our lineage-tracing experiments (Figure 2D).

Additionally, we observed that the loss of EcR and E93 in DL1 NSCs using 17A12-GAL4 also resulted in the mistargeting of axonal projections in the surviving 23E10 dFB neurons. Whereas neurons in control brains extend their axonal projections to the dorsal layer of the FB (Figures 5D and 5D′), those with reduced EcR and E93 expression misproject their axonal projection to the middle and ventral layers of FB (Figures 5E–5F′). This indicates that E93 and EcR have roles beyond merely specifying the 23E10 dFB neurons, suggesting further studies are needed to understand the molecular mechanisms by which EcR and E93 contribute to the CX lineage specification and connectivity.

Type II NSCs begin expressing EcR around ∼55 h ALH, with E93 expression initiating shortly thereafter and peaking at around 120 h ALH and pupae.[15] To refine the developmental timing of E93's function, we focused on the period when 23E10 dFB neurons are generated, between 48 and 76 h ALH. We utilized the temporal and regional gene expression targeting (TARGET) system[129] to restrict E93 knockdown to this specific developmental time (Figures 6A and 6B). Briefly, at the permissive temperature (18°C), GAL80ts is active and inhibits GAL4 activity by binding to its activation domain; this inhibition is released when the temperature shifts to 29°C, allowing GAL4 to function (Figure 6A). Knockdown of E93 starting at 48 h ALH or later significantly decreased the total number of 23E10 dFB neurons, mimicking the phenotype seen with constitutive E93 knockdown (Figures 4C and 4C′). This confirms that the temporal expression of E93 in type II NSCs between 48 and 76 h ALH is crucial for specifying 23E10 dFB neurons. For controls, we used UAS-E93RNAi without GAL80ts and UAS-E93RNAi with GAL80ts, grown at constant temperatures of 29°C and 18°C (Figures 6C–6F′). The quantification of control and experimental animals (Figure 6G) indicates that ecdysone-induced, type-II-NSC-specific temporal expression

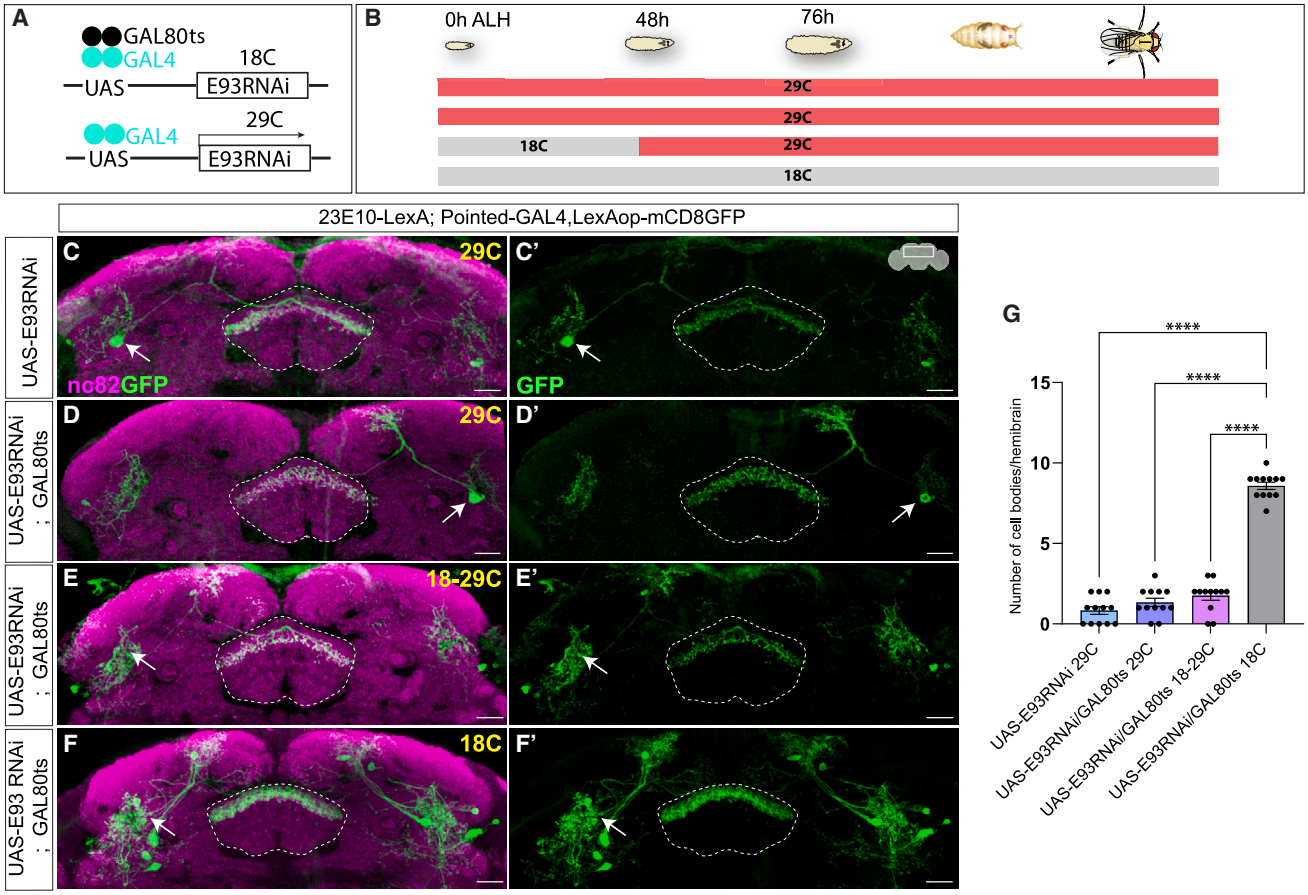

Figure 6. E93 expression in a restricted time window regulates 23E10 dFB neuronal fate

(A) Schematic of TARGET system illustrating GAL80ts-mediated restricted knockdown of E93. At 18°C, GAL80ts is active, preventing the E93 RNAi expression by inhibiting Pointed-GAL4 activity. At 29°C, GAL80ts is inactive, allowing E93 RNAi expression temporally.

(B) Schematic of the experimental setup showing E93 RNAi flies reared at different temperatures throughout the larval life cycle, from 0 to 120 h ALH. Flies with E93 RNAi and GAL80ts were initially grown at 18°C and then shifted to 29°C around 40 h ALH to enable E93 RNAi expression in late type II NSCs.

(C and C′) Shows a loss of 23E10 dFB neurons, labeled with GFP, at 29°C upon E93 knockdown (E93 RNAi without dicer).

(D and D′) Displays loss of 23E10 dFB neurons upon continuous E93 RNAi expression in animals grown at 29°C throughout development (GAL80ts is inactive at 29°C).

(E and E′) Shows significant loss of 23E10 dFB neurons when UAS-E93 RNAi is restricted to late type II NSCs using GAL80ts. Flies were grown at 18°C until 40 h ALH and then shifted to 29°C to inactivate GAL80ts.

(F and F′) The 23E10 dFB neuron number remains normal when flies expressing UAS-E93 RNAi combined with GAL80ts are grown continuously at 18°C.

(G) Quantification of 23E10 dFB neuron cell bodies per hemibrain using one-way ANOVA followed by Dunnett's multiple comparison test. Error bars represent ±SD. Asterisks indicate statistical significance: *$p < 0.05$, **$p < 0.01$, ***$p < 0.001$, **** $p < 0.0001$; NS, non-significant.

Cell bodies are indicated by white arrows. The dashed line outlines the FB.

Scale bars represent 20 μm. $n = 12$ adult hemibrains for each genotype.

of E93 between 48 and 76 h ALH is essential for specifying 23E10 dFB neurons.

Loss of E93 in larval NSCs impairs adult sleep behaviors

The *Drosophila* CX has been implicated as a center for sleep regulation,[36,50–53,58–60,88–90] with evidence of a specific role for the 23E10 dFB in sleep homeostasis.[52,87] We tested whether loss of E93 in type II NSCs affects baseline sleep in adulthood. E93 knockdown in type II NSCs using Pointed-GAL4 had little effect on total sleep duration or sleep continuity (Figures 7A–7D), despite dramatic effects on the 23E10 dFB neuronal fate. This finding is consistent with studies showing that 23E10 dFB neuron inhibition has minimal impact on sleep duration in mature adulthood.[55,92] However, recent evidence indicates that sleep in *Drosophila* is not a homogeneous state and that deeper sleep occurs during periods of consolidated sleep consisting of long sleep bouts.[130–136] Given the proposed role of 23E10+ cells in generating sleep drive, we asked whether long bouts of sleep (60 min or longer) might be selectively affected by E93 knockdown. While the overall duration of sleep composed of these long bouts was unaffected by E93 knockdown (Figures 7E and 7F), we observed a marked reduction of mean bout length and an increase in number during the night (Figures 7G and 7H), which is the period when deep sleep primarily occurs.[130,132,133]

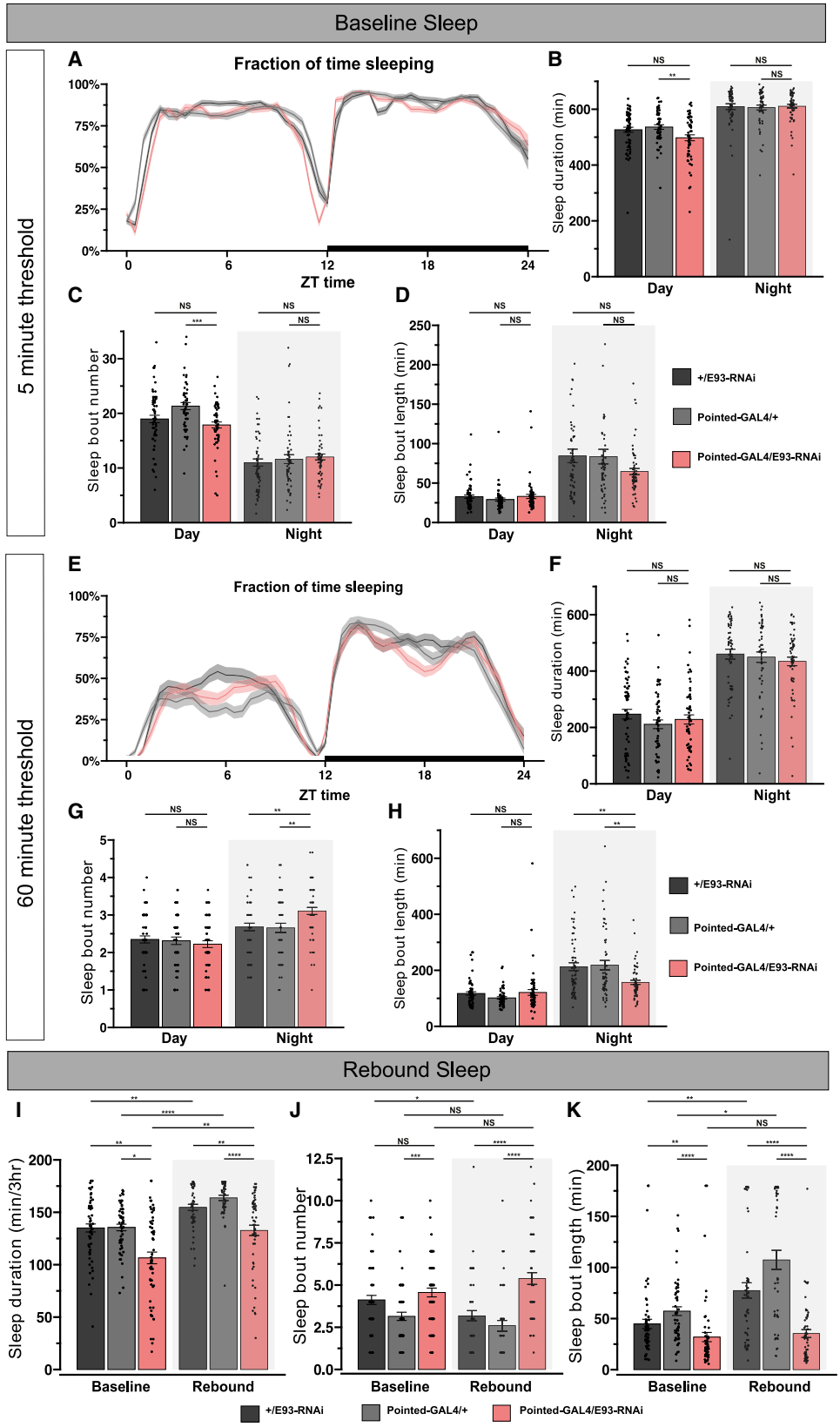

(legend on next page)

These results show that the loss of 23E10 dFB neurons is associated with impairments in deep sleep.

To further probe for an impairment in deep sleep, we next examined how knockdown of E93 in type II NSCs affects sleep rebound following a night of sleep deprivation, which normally generates a high sleep pressure state. We assessed sleep during the first 3 h of the morning on a baseline day and following a night of total sleep deprivation; most sleep is recovered in these first 3 h following sleep deprivation.[55] In these experiments, we detected a decrease in baseline sleep duration during the first 3 h of the day with E93 knockdown (Figure 7I, baseline). Following sleep deprivation, both parental controls and E93 knockdown flies exhibited an increase in sleep amount (Figure 7I, rebound), indicating that sleep rebound can still occur despite the loss of 23E10 dFB neurons. However, sleep during the rebound period was dramatically fragmented (shorter sleep bouts). Sleep-deprived control flies exhibited a near doubling of sleep bout length during the rebound period, reflecting the normal increase in sleep pressure (Figures 7J and 7K). In contrast, sleep bout length in E93 knockdown flies remained unchanged from the baseline period, associated with an increase in bout number compared with controls (Figures 7J and 7K). These findings indicate a failure to achieve consolidated sleep following enforced sleep loss. Notably, recent work has raised the possibility that sleep-relevant neurons labeled by the 23E10 driver reside in the VNC in addition to neurons in the brain.[91,92] We found that E93 knockdown in type II NSCs impairs 23E10 dFB neurons but spares the 23E10+ VNC neurons (Figure S4). Our developmental approach thus supports a brain-specific sleep role for 23E10 dFB neurons in regulating deep sleep in contexts associated with high sleep pressure.

DISCUSSION

Generating complex behaviors requires integrating various sensory modalities to produce motor output in a context-dependent manner. Distinct types of neurons provide unique sensory inputs or modulate motor outputs to regulate behaviors such as navigation, feeding, and sleep. Understanding brain function, therefore, involves investigating developmental programs that establish these circuits and behaviors. Here, we have investigated the lineage-specific development of sleep-regulating neurons that are an essential part of a sleep-wake circuit.[51,53] We identified the NSCs that generate 23E10 dFB neurons in the brain and mapped their birth timing (Figures 2C, 2D, and 2H). Our work has identified the critical role of temporal steroid hormonal signaling in regulating the specification of the 23E10 dFB neurons through E93 (Figures 3 and 4) and demonstrated how E93 in type II NSCs influences adult sleep (Figure 7). This study offers new insights into the genetic and developmental basis of sleep, links sleep behavior to specific NSCs, and provides a developmental perspective that might help resolve the recent controversies in the sleep field.[91,92,95]

From lineages to sleep circuits

Diverse classes of large-field input neurons feed sensory information to the CX by innervating and making connections in the different layers of the FB. Recent connectome data have identified distinct modules within the FB layers that correspond to specific behaviors, with layers 6–7 as a sleep-wake module.[36] The FB, the most diverse structure in the CX, receives input from the periphery via the long-field neurons that innervate its layers in a topographic manner. The FB long-field neurons arise from different NSCs, with significant contributions from the DL1 type II NSC and DALc12v type I NSC.[63,64,68,102] The 23E10 dFB neurons are long-field input neurons that innervate layers six and seven of the FB.[36] What NSC populations make the long-field tangential input neurons of the sleep-wake circuit? Is the lamination of the FB birth order related? This study shows that the dFB neurons originate primarily from type II NSCs, with most derived from DL1 lineages and a few from the DM1 lineage. Previous clonal studies did not assign any contributions of DM1 lineage to the long-field input neurons. However, consistent with our findings, a recent connectomics-based lineage assignment study has also proposed DM1 lineage contribution to the FB tangential input neurons.[102] Although all ~12 neurons look similar in morphology, our clonal analysis data suggest a likely heterogeneity of cells in this cluster. Each neuron in that cluster could be a unique neuron type getting inputs from distinct upstream neurons and part of unique circuits. The connectomics-based studies will help assign unique input and output neurons to these distinct classes of dFB neurons. Furthermore, single-cell RNA sequencing will help delineate the distinct cell types in the dFB cluster.

Are the neuron types innervating distinct FB layers specified at different times during development? Our findings reveal that the sleep-regulating 23E10 dFB neurons are born from the old type II NSCs between 48 and 76 h ALH. Previous studies indicate that large-field tangential input neurons that innervate ventral FB layers are generated only until 72 h ALH, supporting the idea of time-dependent lamination in the FB.[17,128] Once specified, the 23E10 dFB neurons innervate the FB around 48 h APF, where they intermingle with arousal-regulating dopaminergic inputs inputs—a process controlled by post-mitotic expression of the conserved gene pdm3.[56] Further studies focusing on additional neural cell types innervating distinct layers and functioning in discrete neural circuits will be essential to relate time and temporal factors expressed in type II NSCs with the assembly of the circuits in distinct FB layers.

Hormonal regulation of the neural fate

Our study demonstrates that ecdysone signaling, through E93, specifies an essential cell type of the sleep-wake circuit,

Figure 7. Knockdown of E93 in larval type II NSCs impairs adult sleep

Sleep traces (A) and quantification of day and night sleep duration (B), sleep bout number (C), and sleep bout length (D) in flies expressing E93-RNAi under control of Pointed-GAL4 (red) compared with genetic controls (black, gray) using the standard 5-min quiescence threshold for sleep. (E–H) Shows the same data for long-bout sleep (≥60-min quiescence threshold for sleep). n = 60, 55, 59 from left to right (A–H). Quantification of sleep duration (I), sleep bout number (J), and sleep bout length (K) in E93-RNAi flies and controls during the first 3 h of a baseline day or following a night (12 h) of sleep deprivation. n = 51, 47, 57 from left to right. Error bars represent SEM; *p < 0.05, **p < 0.01, ***p < 0.001, ****p < 0.0001; NS, non-significant by Kruskal-Wallis test with Dunn's multiple comparison corrections. See also Figure S4.

revealing a crucial role of developmental hormonal signaling in specifying 23E10 dFB neurons and sleep behavior. These findings link an extrinsic hormonal signal to the stem cell-intrinsic factors that specify neural fate. Ecdysone signaling plays many roles during development, metamorphosis, and post development in regulating various physiological processes.[111,112,137,138] Although ecdysone is present at varying concentrations throughout development, cells respond differentially by expressing unique EcR isoforms over time. Our recent work showed that temporal expression of EcR in type II NSCs around 55 h ALH mediates early to late transition in mid-larval stages.[15] Although most animals show a complete loss of 23E10 dFB neurons upon EcR and E93 knockdown, some animals retain a few neurons that exhibit defective morphology and are mistargeted to incorrect FB layers (Figures 3F–3H′). This suggests that EcR and E93 in type II NSCs are required to regulate 23E10 dFB neuronal fate and their appropriate targeting to FB layers. The inability to rescue the EcR loss-of-function phenotype by E93 indicates that both EcR and E93 are necessary (Figures 4E, 4E′, and 4H). One possible explanation is that ecdysone signaling through EcR is needed to open the chromatin for normal E93 function. Similar sequential gene expression pathways and temporal competence of TFs to function exist in embryonic and optic lobe neuroblasts.[16,139] The FB layers express unique ligand combinations that regulate proper targeting[140]; one possibility is that EcR regulates the layer-specific expression of cell adhesion molecules or their receptors in neurons. More studies are needed to elucidate how EcR and ecdysone signaling regulate CX development.

How does E93 regulate cell fate? Ecdysone-induced protein E93 regulates multiple developmental processes, from wing disc growth to NSC apoptosis.[111,120,141–144] In developing wing discs, E93 functions as a chromatin remodeler, activating or repressing genes by opening and closing chromatin.[143] Further work on identifying E93 targets will clarify its role in type II NSCs. Overexpression of E93 in young NSCs did not increase the number of 23E10 dFB neurons, indicating that E93 alone is insufficient for their specification; a combination of TFs may be needed. Additionally, ectopic E93 expression failed to induce 23E10 dFB neurons in other type II lineages, suggesting the presence of an unknown spatial factor specific to DL1 NSCs. It is possible that ectopically expressed E93 cannot function in the young NSCs and can only act in the later periods after EcR expression. Previous studies[143] in *Drosophila* wing discs have shown that not all genomic targets respond to a precocious expression of E93 at all stages, implying that additional temporal factors may be required. We speculate that temporal hormonal signaling might alter the chromatin landscape of the late type II NSCs—as a result, the early/late factors have differential access to the chromatin and thus specify fate by different genes. It would be interesting to investigate the targets of the EcR and E93 in the type II NSCs and the 23E10 dFB neurons. In post-mitotic neurons, E93 may regulate a set of effector genes required for consolidating and maintaining 23E10 dFB neuronal identity, similar to the terminal selector genes that govern the expression of effector genes, endowing neurons with unique properties.[145–148] Given that ecdysone and E93 regulate various developmental processes in insects,[111,120,144,149] it would be intriguing to explore whether E93 regulates the development of tangential input neurons in other insect species.

Hormonal regulation of sleep behavior

How do developmental hormonal cues specify sleep behavior? Previous studies have reported a role of ecdysone signaling in regulating adult sleep behavior.[150–152] Whole-animal ecdysone and EcR hypomorph mutants show adult sleep pattern defects.[150,151] Recently, EcR expression in cortex glia has been implicated in regulating sleep architecture.[152] Our data point to a role for developmental hormonal signaling in adult sleep in a cell-type-specific manner via the generation of 23E10 dFB sleep neurons. While evidence over the past decade supports a role for these cells in sleep,[50–53,58] studies have suggested that inhibition of these cells has little impact on daily sleep duration in mature adulthood[55,92,95] and raises the possibility that the sleep-regulating effect of 23E10+ neuronal activation includes cells outside the brain.[91,92]

Our developmental manipulations contribute further to the apparent complexity of the CX in sleep regulation. E93 knockdown in type II NSCs causes gross abnormalities in 23E10 dFB development and morphology while sparing 23E10+ VNC neurons. Although baseline adult sleep duration is largely intact, a proxy for deep sleep (long sleep bouts) is impaired during the night, and sleep homeostasis is disrupted. The nuanced sleep phenotypes with loss of these cells are consistent with a highly specialized role for dFB in sleep regulation. Recent studies demonstrate that 23E10-labeled neurons that project to dFB are heterogeneous both from a neurochemical[95] and transcriptional[94] perspective and that only a small subset of these dFB neurons are relevant for sleep.[94] Additionally, specific optical stimulation paradigms of these cells are required to induce sleep.[94,95] Yet, our results support the hypothesis that the 23E10-labeled dFB cluster does indeed contain sleep-relevant neurons, but not necessarily with a prominent role in daily sleep control. Rather, this sleep region of the brain appears to be most relevant in conditions when the drive to sleep is heightened, such as after sleep deprivation. These findings underscore how detailed insights into sleep circuit lineages and development can inform adult sleep-regulatory mechanisms.

RESOURCE AVAILABILITY

Lead contact

Further information and requests for resources and reagents should be directed to and will be fulfilled by the lead contact, Mubarak Hussain Syed (flyguy@unm.edu).

Materials availability

This study did not generate new unique reagents. Requests of fly stocks should be directed to and will be fulfilled by the lead contact, Mubarak Hussain Syed (flyguy@unm.edu).

Data and code availability

- All data are presented in Figures 1, 2, 3, 4, 5, 6, 7, and S1–S4 of this paper. The raw data used to generate figures in this study will be publicly available at https://osf.io/xkmwf/.
- This paper does not report the original code.
- Any additional information required to reanalyze the data reported in this paper is available from the lead contact upon request.

ACKNOWLEDGMENTS

The authors thank Chris Doe, Doe lab, and Neural Diversity lab members for their valuable feedback and discussions. We thank Chris Doe and Asif Bakshi

for providing critical feedback on the manuscript. We are grateful to Tzumin Lee, Chris Doe, Claude Desplan, Cheng-Yu Lee, and Gerry Rubin for sharing the reagents. Stocks obtained from the Bloomington Drosophila Stock Center (NIH P40OD018537) were used in this study. The monoclonal nc82 antibody was obtained from the Developmental Studies Hybridoma Bank, created by the NICHD of the NIH and maintained at The University of Iowa, Department of Biology, Iowa City, IA 52242. We thank UNM Biology Cell Biology Core for providing the confocal microscopy facility and Janelia Research Campus/HHMI for donating Zeiss LSM 710, which was used for imaging during the review process. The Company of Biologists Travelling Fellowship to A.R.W., the Arnold O. Beckman Postdoctoral Fellowship to J.I.-B. The research was supported by NIH DP2NS111996 and NIH R01NS120979 to M.S.K. and through the National Science Foundation CAREER Award IOS-2047020, Sloan Research Fellowship FG-2023-20617, 2023 BBRF Young Investigator Grant, and McKnight Scholars Award to M.H.S.

AUTHOR CONTRIBUTIONS

Conceptualization, A.R.W., M.S.K., and M.H.S.; methodology, A.R.W. performed all genetics, anatomy experiments, and confocal imaging with help from G.M.C. K.P. performed initial sleep experiments; B.C. and J.L. performed sleep behavior experiments under the supervision of M.S.K.; J.I.-B. provided the FLPStop2.0 construct and helped design the strategy to generate EcR-FLPStop2.0 flies; visualization, A.R.W., M.S.K., and M.H.S.; writing – original draft, A.R.W. and M.H.S.; editing, A.R.W., B.C., M.S.K., and M.H.S.; funding acquisition, M.S.K. and M.H.S.; and supervision, M.S.K. and M.H.S.

DECLARATION OF INTERESTS

The authors declare no competing interests.

STAR★METHODS

Detailed methods are provided in the online version of this paper and include the following:

- KEY RESOURCES TABLE
- EXPERIMENTAL MODEL AND SUBJECT DETAILS
- METHOD DETAILS
  - Immunostaining
  - Microscopy
  - Clonal analysis and birthdating
  - Generation of FLPStop2.0 plasmid for transgenesis
  - Generation of FLPStop2.0 transgenic flies
  - Sleep assays
- QUANTIFICATION AND STATISTICAL ANALYSIS

SUPPLEMENTAL INFORMATION

Supplemental information can be found online at https://doi.org/10.1016/j.cub.2024.09.020.

Received: September 21, 2023
Revised: August 9, 2024
Accepted: September 11, 2024
Published: October 8, 2024

REFERENCES

1. Kohwi, M., and Doe, C.Q. (2013). Temporal Fate Specification and Neural Progenitor Competence During Development. Nat. Rev. Neurosci. *14*, 823–838. https://doi.org/10.1038/nrn3618.
2. Molnár, Z., Clowry, G.J., Šestan, N., Alzu'bi, A., Bakken, T., Hevner, R.F., Hüppi, P.S., Kostović, I., Rakic, P., Anton, E.S., et al. (2019). New insights into the development of the human cerebral cortex. J. Anat. *235*, 432–451. https://doi.org/10.1111/joa.13055.
3. Oberst, P., Agirman, G., and Jabaudon, D. (2019). Principles of progenitor temporal patterning in the developing invertebrate and vertebrate nervous system. Curr. Opin. Neurobiol. *56*, 185–193. https://doi.org/10.1016/j.conb.2019.03.004.
4. El-Danaf, R.N., Rajesh, R., and Desplan, C. (2023). Temporal regulation of neural diversity in Drosophila and vertebrates. Semin. Cell Dev. Biol. *142*, 13–22. https://doi.org/10.1016/j.semcdb.2022.05.011.
5. Malin, J., and Desplan, C. (2021). Neural specification, targeting, and circuit formation during visual system assembly. Proc. Natl. Acad. Sci. USA *118*, e2101823118. https://doi.org/10.1073/pnas.2101823118.
6. Doe, C.Q. (2017). Temporal Patterning in the Drosophila CNS. Annu. Rev. Cell Dev. Biol. *33*, 219–240. https://doi.org/10.1146/annurev-cellbio-111315-125210.
7. Hamid, A., Gutierrez, A., Munroe, J., and Syed, M.H. (2023). The Drivers of Diversity: Integrated genetic and hormonal cues regulate neural diversity. Semin. Cell Dev. Biol. *142*, 23–35. https://doi.org/10.1016/j.semcdb.2022.07.007.
8. Koo, B., Lee, K.-H., Ming, G.-L., Yoon, K.-J., and Song, H. (2023). Setting the clock of neural progenitor cells during mammalian corticogenesis. Semin. Cell Dev. Biol. *142*, 43–53. https://doi.org/10.1016/j.semcdb.2022.05.013.
9. Sen, S.Q., Chanchani, S., Southall, T.D., and Doe, C.Q. (2019). Neuroblast-specific open chromatin allows the temporal transcription factor, Hunchback, to bind neuroblast-specific loci. eLife *8*, e44036. https://doi.org/10.7554/eLife.44036.
10. Sen, S.Q. (2023). Generating neural diversity through spatial and temporal patterning. Semin. Cell Dev. Biol. *142*, 54–66. https://doi.org/10.1016/j.semcdb.2022.06.002.
11. Erclik, T., Li, X., Courgeon, M., Bertet, C., Chen, Z., Baumert, R., Ng, J., Koo, C., Arain, U., Behnia, R., et al. (2017). Integration of temporal and spatial patterning generates neural diversity. Nature *541*, 365–370. https://doi.org/10.1038/nature20794.
12. Chen, Y.-C., and Konstantinides, N. (2022). Integration of Spatial and Temporal Patterning in the Invertebrate and Vertebrate Nervous System. Front. Neurosci. *16*, 854422. https://doi.org/10.3389/fnins.2022.854422.
13. Guillemot, F. (2007). Spatial and temporal specification of neural fates by transcription factor codes. Development *134*, 3771–3780. https://doi.org/10.1242/dev.006379.
14. Isshiki, T., Pearson, B., Holbrook, S., and Doe, C.Q. (2001). Drosophila neuroblasts sequentially express transcription factors which specify the temporal identity of their neuronal progeny. Cell *106*, 511–521. https://doi.org/10.1016/s0092-8674(01)00465-2.
15. Syed, M.H., Mark, B., and Doe, C.Q. (2017). Steroid hormone induction of temporal gene expression in Drosophila brain neuroblasts generates neuronal and glial diversity. eLife *6*, e26287. https://doi.org/10.7554/eLife.26287.
16. Li, X., Erclik, T., Bertet, C., Chen, Z., Voutev, R., Venkatesh, S., Morante, J., Celik, A., and Desplan, C. (2013). Temporal patterning of Drosophila medulla neuroblasts controls neural fates. Nature *498*, 456–462. https://doi.org/10.1038/nature12319.
17. Ren, Q., Yang, C.-P., Liu, Z., Sugino, K., Mok, K., He, Y., Ito, M., Nern, A., Otsuna, H., and Lee, T. (2017). Stem Cell-Intrinsic, Seven-up-Triggered Temporal Factor Gradients Diversify Intermediate Neural Progenitors. Curr. Biol. *27*, 1303–1313. https://doi.org/10.1016/j.cub.2017.03.047.
18. Liu, Z., Yang, C.-P., Sugino, K., Fu, C.-C., Liu, L.-Y., Yao, X., Lee, L.P., and Lee, T. (2015). Opposing intrinsic temporal gradients guide neural stem cell production of varied neuronal fates. Science *350*, 317–320. https://doi.org/10.1126/science.aad1886.
19. Maurange, C., Cheng, L., and Gould, A.P. (2008). Temporal Transcription Factors and Their Targets Schedule the End of Neural Proliferation in Drosophila. Cell *133*, 891–902. https://doi.org/10.1016/j.cell.2008.03.034.

20. Alsiö, J.M., Tarchini, B., Cayouette, M., and Livesey, F.J. (2013). Ikaros promotes early-born neuronal fates in the cerebral cortex. Proc. Natl. Acad. Sci. USA *110*, E716–E725. https://doi.org/10.1073/pnas.1215707110.

21. Elliott, J., Jolicoeur, C., Ramamurthy, V., and Cayouette, M. (2008). Ikaros Confers Early Temporal Competence to Mouse Retinal Progenitor Cells. Neuron *60*, 26–39. https://doi.org/10.1016/j.neuron.2008.08.008.

22. Mattar, P., Jolicoeur, C., Dang, T., Shah, S., Clark, B.S., and Cayouette, M. (2021). A Casz1–NuRD complex regulates temporal identity transitions in neural progenitors. Sci. Rep. *11*, 3858. https://doi.org/10.1038/s41598-021-83395-7.

23. Dias, J.M., Alekseenko, Z., Applequist, J.M., and Ericson, J. (2014). Tgfβ Signaling Regulates Temporal Neurogenesis and Potency of Neural Stem Cells in the CNS. Neuron *84*, 927–939. https://doi.org/10.1016/j.neuron.2014.10.033.

24. Telley, L., Agirman, G., Prados, J., Amberg, N., Fièvre, S., Oberst, P., Bartolini, G., Vitali, I., Cadilhac, C., Hippenmeyer, S., et al. (2019). Temporal patterning of apical progenitors and their daughter neurons in the developing neocortex. Science *364*, eaav2522. https://doi.org/10.1126/science.aav2522.

25. Sagner, A., Zhang, I., Watson, T., Lazaro, J., Melchionda, M., and Briscoe, J. (2021). A shared transcriptional code orchestrates temporal patterning of the central nervous system. PLoS Biol. *19*, e3001450. https://doi.org/10.1371/journal.pbio.3001450.

26. Lodato, S., and Arlotta, P. (2015). Generating Neuronal Diversity in the Mammalian Cerebral Cortex. Annu. Rev. Cell Dev. Biol. *31*, 699–720. https://doi.org/10.1146/annurev-cellbio-100814-125353.

27. Sagner, A., and Briscoe, J. (2019). Establishing neuronal diversity in the spinal cord: a time and a place. Development *146*, dev182154. https://doi.org/10.1242/dev.182154.

28. Honkanen, A., Adden, A., da Silva Freitas, J.da S., and Heinze, S. (2019). The insect central complex and the neural basis of navigational strategies. J. Exp. Biol. *222*, jeb188854. https://doi.org/10.1242/jeb.188854.

29. Pfeiffer, K., and Homberg, U. (2014). Organization and Functional Roles of the Central Complex in the Insect Brain. Annu. Rev. Entomol. *59*, 165–184. https://doi.org/10.1146/annurev-ento-011613-162031.

30. Turner-Evans, D.B., and Jayaraman, V. (2016). The insect central complex. Curr. Biol. *26*, R453–R457. https://doi.org/10.1016/j.cub.2016.04.006.

31. Seelig, J.D., and Jayaraman, V. (2015). Neural dynamics for landmark orientation and angular path integration. Nature *521*, 186–191. https://doi.org/10.1038/nature14446.

32. Lu, J., Behbahani, A.H., Hamburg, L., Westeinde, E.A., Dawson, P.M., Lyu, C., Maimon, G., Dickinson, M.H., Druckmann, S., and Wilson, R.I. (2022). Transforming representations of movement from body- to world-centric space. Nature *601*, 98–104. https://doi.org/10.1038/s41586-021-04191-x.

33. Lyu, C., Abbott, L.F., and Maimon, G. (2022). Building an allocentric travelling direction signal via vector computation. Nature *601*, 92–97. https://doi.org/10.1038/s41586-021-04067-0.

34. Fisher, Y.E. (2022). Flexible navigational computations in the Drosophila central complex. Curr. Opin. Neurobiol. *73*, 102514. https://doi.org/10.1016/j.conb.2021.12.001.

35. Turner-Evans, D.B., Jensen, K.T., Ali, S., Paterson, T., Sheridan, A., Ray, R.P., Wolff, T., Lauritzen, J.S., Rubin, G.M., Bock, D.D., et al. (2020). The Neuroanatomical Ultrastructure and Function of a Biological Ring Attractor. Neuron *108*, 145–163.e10. https://doi.org/10.1016/j.neuron.2020.08.006.

36. Hulse, B.K., Haberkern, H., Franconville, R., Turner-Evans, D.B., Takemura, S.-Y., Wolff, T., Noorman, M., Dreher, M., Dan, C., Parekh, R., et al. (2021). A connectome of the Drosophila central complex reveals network motifs suitable for flexible navigation and context-dependent action selection. eLife *10*, e66039. https://doi.org/10.7554/eLife.66039.

37. Heinze, S., Narendra, A., and Cheung, A. (2018). Principles of Insect Path Integration. Curr. Biol. *28*, R1043–R1058. https://doi.org/10.1016/j.cub.2018.04.058.

38. Dacke, M., Baird, E., el Jundi, B., Warrant, E.J., and Byrne, M. (2021). How Dung Beetles Steer Straight. Annu. Rev. Entomol. *66*, 243–256. https://doi.org/10.1146/annurev-ento-042020-102149.

39. Collett, M., Chittka, L., and Collett, T.S. (2013). Spatial Memory in Insect Navigation. Curr. Biol. *23*, R789–R800. https://doi.org/10.1016/j.cub.2013.07.020.

40. Sayre, M.E., Templin, R., Chavez, J., Kempenaers, J., and Heinze, S. (2021). A projectome of the bumblebee central complex. eLife *10*, e68911. https://doi.org/10.7554/eLife.68911.

41. Strauss, R. (2002). The central complex and the genetic dissection of locomotor behaviour. Curr. Opin. Neurobiol. *12*, 633–638. https://doi.org/10.1016/s0959-4388(02)00385-9.

42. Strausfeld, N.J. (1999). Chapter 24 A. Brain Region in Insects That Supervises Walking. In Progress in Brain Research Peripheral and Spinal Mechanisms in the Neural Control of Movement, M.D. Binder, ed. (Elsevier), pp. 273–284. https://doi.org/10.1016/S0079-6123(08)62863-0.

43. Martin, J.R., Raabe, T., and Heisenberg, M. (1999). Central complex substructures are required for the maintenance of locomotor activity in Drosophila melanogaster. J. Comp. Physiol. A *185*, 277–288. https://doi.org/10.1007/s003590050387.

44. Strauss, R., and Heisenberg, M. (1993). A higher control center of locomotor behavior in the Drosophila brain. J. Neurosci. *13*, 1852–1861. https://doi.org/10.1523/JNEUROSCI.13-05-01852.1993.

45. Bender, J.A., Pollack, A.J., and Ritzmann, R.E. (2010). Neural activity in the central complex of the insect brain is linked to locomotor changes. Curr. Biol. *20*, 921–926. https://doi.org/10.1016/j.cub.2010.03.054.

46. Martin, J.P., Guo, P., Mu, L., Harley, C.M., and Ritzmann, R.E. (2015). Central-complex control of movement in the freely walking cockroach. Curr. Biol. *25*, 2795–2803. https://doi.org/10.1016/j.cub.2015.09.044.

47. Sareen, P.F., McCurdy, L.Y., and Nitabach, M.N. (2021). A neuronal ensemble encoding adaptive choice during sensory conflict in Drosophila. Nat. Commun. *12*, 4131. https://doi.org/10.1038/s41467-021-24423-y.

48. Musso, P.-Y., Junca, P., and Gordon, M.D. (2021). A neural circuit linking two sugar sensors regulates satiety-dependent fructose drive in Drosophila. Sci. Adv. *7*, eabj0186. https://doi.org/10.1126/sciadv.abj0186.

49. Ni, J.D., Gurav, A.S., Liu, W., Ogunmowo, T.H., Hackbart, H., Elsheikh, A., Verdegaal, A.A., and Montell, C. (2019). Differential regulation of the Drosophila sleep homeostat by circadian and arousal inputs. eLife *8*, e40487. https://doi.org/10.7554/eLife.40487.

50. Donlea, J.M., Thimgan, M.S., Suzuki, Y., Gottschalk, L., and Shaw, P.J. (2011). Inducing sleep by remote control facilitates memory consolidation in Drosophila. Science *332*, 1571–1576. https://doi.org/10.1126/science.1202249.

51. Pimentel, D., Donlea, J.M., Talbot, C.B., Song, S.M., Thurston, A.J.F., and Miesenböck, G. (2016). Operation of a homeostatic sleep switch. Nature *536*, 333–337. https://doi.org/10.1038/nature19055.

52. Donlea, J.M., Pimentel, D., and Miesenböck, G. (2014). Neuronal Machinery of Sleep Homeostasis in Drosophila. Neuron *81*, 860–872. https://doi.org/10.1016/j.neuron.2013.12.013.

53. Donlea, J.M., Pimentel, D., Talbot, C.B., Kempf, A., Omoto, J.J., Hartenstein, V., and Miesenböck, G. (2018). Recurrent Circuitry for Balancing Sleep Need and Sleep. Neuron *97*, 378–389.e4. https://doi.org/10.1016/j.neuron.2017.12.016.

54. Kayser, M.S., Yue, Z., and Sehgal, A. (2014). A critical period of sleep for development of courtship circuitry and behavior in Drosophila. Science *344*, 269–274. https://doi.org/10.1126/science.1250553.

55. Gong, N.N., Luong, H.N.B., Dang, A.H., Mainwaring, B., Shields, E., Schmeckpeper, K., Bonasio, R., and Kayser, M.S. (2022). Intrinsic maturation of sleep output neurons regulates sleep ontogeny in Drosophila. Curr. Biol. *32*, 4025–4039.e3. https://doi.org/10.1016/j.cub.2022.07.054.

56. Chakravarti Dilley, L., Szuperak, M., Gong, N.N., Williams, C.E., Saldana, R.L., Garbe, D.S., Syed, M.H., Jain, R., and Kayser, M.S. (2020). Identification of a molecular basis for the juvenile sleep state. eLife *9*, e52676. https://doi.org/10.7554/eLife.52676.

57. Liu, Q., Liu, S., Kodama, L., Driscoll, M.R., and Wu, M.N. (2012). Two Dopaminergic Neurons Signal to the Dorsal Fan-Shaped Body to Promote Wakefulness in Drosophila. Curr. Biol. *22*, 2114–2123. https://doi.org/10.1016/j.cub.2012.09.008.

58. Ueno, T., Tomita, J., Tanimoto, H., Endo, K., Ito, K., Kume, S., and Kume, K. (2012). Identification of a dopamine pathway that regulates sleep and arousal in Drosophila. Nat. Neurosci. *15*, 1516–1523. https://doi.org/10.1038/nn.3238.

59. Liu, S., Liu, Q., Tabuchi, M., and Wu, M.N. (2016). Sleep Drive Is Encoded by Neural Plastic Changes in a Dedicated Circuit. Cell *165*, 1347–1360. https://doi.org/10.1016/j.cell.2016.04.013.

60. Shafer, O.T., and Keene, A.C. (2021). The Regulation of Drosophila Sleep. Curr. Biol. *31*, R38–R49. https://doi.org/10.1016/j.cub.2020.10.082.

61. Wolff, T., Iyer, N.A., and Rubin, G.M. (2015). Neuroarchitecture and neuroanatomy of the *Drosophila* central complex: A GAL4-based dissection of protocerebral bridge neurons and circuits. J. Comp. Neurol. *523*, 997–1037. https://doi.org/10.1002/cne.23705.

62. Hanesch, U., Fischbach, K.-F., and Heisenberg, M. (1989). Neuronal architecture of the central complex in Drosophila melanogaster. Cell Tissue Res. *257*, 343–366. https://doi.org/10.1007/BF00261838.

63. Yu, H.-H., Awasaki, T., Schroeder, M.D., Long, F., Yang, J.S., He, Y., Ding, P., Kao, J.-C., Wu, G.Y.-Y., Peng, H., et al. (2013). Clonal development and organization of the adult Drosophila central brain. Curr. Biol. *23*, 633–643. https://doi.org/10.1016/j.cub.2013.02.057.

64. Yang, J.S., Awasaki, T., Yu, H.-H., He, Y., Ding, P., Kao, J.-C., and Lee, T. (2013). Diverse neuronal lineages make stereotyped contributions to the Drosophila locomotor control center, the central complex. J. Comp. Neurol. *521*, 2645–Spc1. https://doi.org/10.1002/cne.23339.

65. Bayraktar, O.A., and Doe, C.Q. (2013). Combinatorial temporal patterning in progenitors expands neural diversity. Nature *498*, 449–455. https://doi.org/10.1038/nature12266.

66. Izergina, N., Balmer, J., Bello, B., and Reichert, H. (2009). Postembryonic development of transit amplifying neuroblast lineages in the Drosophila brain. Neural Dev. *4*, 44. https://doi.org/10.1186/1749-8104-4-44.

67. Viktorin, G., Riebli, N., Popkova, A., Giangrande, A., and Reichert, H. (2011). Multipotent neural stem cells generate glial cells of the central complex through transit amplifying intermediate progenitors in Drosophila brain development. Dev. Biol. *356*, 553–565. https://doi.org/10.1016/j.ydbio.2011.06.013.

68. Ito, M., Masuda, N., Shinomiya, K., Endo, K., and Ito, K. (2013). Systematic analysis of neural projections reveals clonal composition of the Drosophila brain. Curr. Biol. *23*, 644–655. https://doi.org/10.1016/j.cub.2013.03.015.

69. Bello, B.C., Izergina, N., Caussinus, E., and Reichert, H. (2008). Amplification of neural stem cell proliferation by intermediate progenitor cells in Drosophila brain development. Neural Dev. *3*, 5. https://doi.org/10.1186/1749-8104-3-5.

70. Boone, J.Q., and Doe, C.Q. (2008). Identification of Drosophila type II neuroblast lineages containing transit amplifying ganglion mother cells. Dev. Neurobiol. *68*, 1185–1195. https://doi.org/10.1002/dneu.20648.

71. Bowman, S.K., Rolland, V., Betschinger, J., Kinsey, K.A., Emery, G., and Knoblich, J.A. (2008). The Tumor Suppressors Brat and Numb Regulate Transit-Amplifying Neuroblast Lineages in Drosophila. Dev. Cell *14*, 535–546. https://doi.org/10.1016/j.devcel.2008.03.004.

72. Wang, Y.-C., Yang, J.S., Johnston, R., Ren, Q., Lee, Y.-J., Luan, H., Brody, T., Odenwald, W.F., and Lee, T. (2014). Drosophila intermediate neural progenitors produce lineage-dependent related series of diverse neurons. Development *141*, 253–258. https://doi.org/10.1242/dev.103069.

73. Pebworth, M.-P., Ross, J., Andrews, M., Bhaduri, A., and Kriegstein, A.R. (2021). Human intermediate progenitor diversity during cortical development. Proc. Natl. Acad. Sci. USA *118*, e2019415118. https://doi.org/10.1073/pnas.2019415118.

74. Florio, M., and Huttner, W.B. (2014). Neural progenitors, neurogenesis and the evolution of the neocortex. Development *141*, 2182–2194. https://doi.org/10.1242/dev.090571.

75. Fietz, S.A., Kelava, I., Vogt, J., Wilsch-Bräuninger, M., Stenzel, D., Fish, J.L., Corbeil, D., Riehn, A., Distler, W., Nitsch, R., et al. (2010). OSVZ progenitors of human and ferret neocortex are epithelial-like and expand by integrin signaling. Nat. Neurosci. *13*, 690–699. https://doi.org/10.1038/nn.2553.

76. Hansen, D.V., Lui, J.H., Parker, P.R.L., and Kriegstein, A.R. (2010). Neurogenic radial glia in the outer subventricular zone of human neocortex. Nature *464*, 554–561. https://doi.org/10.1038/nature08845.

77. Boyan, G.S., and Reichert, H. (2011). Mechanisms for complexity in the brain: generating the insect central complex. Trends Neurosci. *34*, 247–257. https://doi.org/10.1016/j.tins.2011.02.002.

78. Boyan, G., and Liu, Y. (2014). Timelines in the insect brain: fates of identified neural stem cells generating the central complex in the grasshopper Schistocerca gregaria. Dev. Genes Evol. *224*, 37–51. https://doi.org/10.1007/s00427-013-0462-8.

79. Ludwig, P., Williams, J.L., Lodde, E., Reichert, H., and Boyan, G.S. (1999). Neurogenesis in the median domain of the embryonic brain of the grasshopper Schistocerca gregaria. J. Comp. Neurol. *414*, 379–390. https://doi.org/10.1002/(SICI)1096-9861(19991122)414:3<379::AID-CNE7>3.0.CO;2-5.

80. Boyan, G.S., and Williams, J.L.D. (1997). Embryonic development of the pars intercerebralis/central complex of the grasshopper. Dev. Genes Evol. *207*, 317–329. https://doi.org/10.1007/s004270050119.

81. Williams, J.L.D., and Boyan, G.S. (2008). Building the central complex of the grasshopper Schistocerca gregaria: axons pioneering the w, x, y, z tracts project onto the primary commissural fascicle of the brain. Arthropod Struct. Dev. *37*, 129–140. https://doi.org/10.1016/j.asd.2007.05.005.

82. Boyan, G., Liu, Y., Khalsa, S.K., and Hartenstein, V. (2017). A conserved plan for wiring up the fan-shaped body in the grasshopper and Drosophila. Dev. Genes Evol. *227*, 253–269. https://doi.org/10.1007/s00427-017-0587-2.

83. Farnworth, M.S., Eckermann, K.N., and Bucher, G. (2020). Sequence heterochrony led to a gain of functionality in an immature stage of the central complex: A fly–beetle insight. PLoS Biol. *18*, e3000881. https://doi.org/10.1371/journal.pbio.3000881.

84. Farnworth, M.S., Bucher, G., and Hartenstein, V. (2022). An atlas of the developing Tribolium castaneum brain reveals conservation in anatomy and divergence in timing to Drosophila melanogaster. J. Comp. Neurol. *530*, 2335–2371. https://doi.org/10.1002/cne.25335.

85. Keene, A.C., and Duboue, E.R. (2018). The origins and evolution of sleep. J. Exp. Biol. *221*, jeb159533. https://doi.org/10.1242/jeb.159533.

86. Helfrich-Förster, C. (2018). Sleep in Insects. Annu. Rev. Entomol. *63*, 69–86. https://doi.org/10.1146/annurev-ento-020117-043201.

87. Qian, Y., Cao, Y., Deng, B., Yang, G., Li, J., Xu, R., Zhang, D., Huang, J., and Rao, Y. (2017). Sleep homeostasis regulated by 5HT2b receptor in a small subset of neurons in the dorsal fan-shaped body of drosophila. eLife *6*, e26519. https://doi.org/10.7554/eLife.26519.

88. Yan, W., Lin, H., Yu, J., Wiggin, T.D., Wu, L., Meng, Z., Liu, C., and Griffith, L.C. (2023). Subtype-Specific Roles of Ellipsoid Body Ring Neurons in Sleep Regulation in Drosophila. J. Neurosci. *43*, 764–786. https://doi.org/10.1523/JNEUROSCI.1350-22.2022.

89. Tomita, J., Ban, G., Kato, Y.S., and Kume, K. (2021). Protocerebral Bridge Neurons That Regulate Sleep in Drosophila melanogaster. Front. Neurosci. *15*, 647117. https://doi.org/10.3389/fnins.2021.647117.

90. Singh, P., Aleman, A., Omoto, J.J., Nguyen, B.-C., Kandimalla, P., Hartenstein, V., and Donlea, J.M. (2023). Examining sleep modulation by Drosophila ellipsoid body neurons. eNeuro *10*, ENEURO.0281-23.2023. https://doi.org/10.1523/ENEURO.0281-23.2023.

91. Jones, J.D., Holder, B.L., Eiken, K.R., Vogt, A., Velarde, A.I., Elder, A.J., McEllin, J.A., and Dissel, S. (2023). Regulation of sleep by cholinergic neurons located outside the central brain in Drosophila. PLoS Biol. *21*, e3002012. https://doi.org/10.1371/journal.pbio.3002012.

92. De, J., Wu, M., Lambatan, V., Hua, Y., and Joiner, W.J. (2023). Re-examining the role of the dorsal fan-shaped body in promoting sleep in Drosophila. Curr. Biol. *33*, 3660–3668.e4. https://doi.org/10.1016/j.cub.2023.07.043.

93. Hasenhuetl, P.S., Sarnataro, R., Vrontou, E., Rorsman, H.O., Talbot, C.B., Brain, R., and Miesenböck, G. (2024). A half-centre oscillator encodes sleep pressure. Preprint at bioRxiv. https://doi.org/10.1101/2024.02.23.581780.

94. Sarnataro, R., Velasco, C.D., Monaco, N., Kempf, A., and Miesenböck, G. (2024). Mitochondrial origins of the pressure to sleep. Preprint at bioRxiv. https://doi.org/10.1101/2024.02.23.581770.

95. Jones, J.D., Holder, B.L., Montgomery, A.C., McAdams, C.V., He, E., Burns, A.E., Eiken, K.R., Vogt, A., Velarde, A.I., Elder, A.J., et al. (2024). The dorsal fan-shaped body is a neurochemically heterogeneous sleep-regulating center in Drosophila. Preprint at bioRxiv. https://doi.org/10.1101/2024.04.10.588925.

96. Doldur-Balli, F., Imamura, T., Veatch, O.J., Gong, N.N., Lim, D.C., Hart, M.P., Abel, T., Kayser, M.S., Brodkin, E.S., and Pack, A.I. (2022). Synaptic dysfunction connects autism spectrum disorder and sleep disturbances: A perspective from studies in model organisms. Sleep Med. Rev. *62*, 101595. https://doi.org/10.1016/j.smrv.2022.101595.

97. Robinson-Shelton, A., and Malow, B.A. (2016). Sleep Disturbances in Neurodevelopmental Disorders. Curr. Psychiatry Rep. *18*, 6. https://doi.org/10.1007/s11920-015-0638-1.

98. Baker, E.K., and Richdale, A.L. (2015). Sleep Patterns in Adults with a Diagnosis of High-Functioning Autism Spectrum Disorder. Sleep *38*, 1765–1774. https://doi.org/10.5665/sleep.5160.

99. Angriman, M., Caravale, B., Novelli, L., Ferri, R., and Bruni, O. (2015). Sleep in children with neurodevelopmental disabilities. Neuropediatrics *46*, 199–210. https://doi.org/10.1055/s-0035-1550151.

100. Abel, E.A., and Tonnsen, B.L. (2017). Sleep phenotypes in infants and toddlers with neurogenetic syndromes. Sleep Med. *38*, 130–134. https://doi.org/10.1016/j.sleep.2017.07.014.

101. Veatch, O.J., Maxwell-Horn, A.C., and Malow, B.A. (2015). Sleep in Autism Spectrum Disorders. Curr. Sleep Med. Rep. *1*, 131–140. https://doi.org/10.1007/s40675-015-0012-1.

102. Kandimalla, P., Omoto, J.J., Hong, E.J., and Hartenstein, V. (2023). Lineages to circuits: the developmental and evolutionary architecture of information channels into the central complex. J. Comp. Physiol. A Neuroethol. Sens. Neural Behav. Physiol. *209*, 679–720. https://doi.org/10.1007/s00359-023-01616-y.

103. Ren, Q., Awasaki, T., Huang, Y.-F., Liu, Z., and Lee, T. (2016). Cell Class-Lineage Analysis Reveals Sexually Dimorphic Lineage Compositions in the Drosophila Brain. Curr. Biol. *26*, 2583–2593. https://doi.org/10.1016/j.cub.2016.07.086.

104. Lee, T. (2017). Wiring the Drosophila Brain with Individually Tailored Neural Lineages. Curr. Biol. *27*, R77–R82. https://doi.org/10.1016/j.cub.2016.12.026.

105. Homem, C.C.F., and Knoblich, J.A. (2012). Drosophila neuroblasts: a model for stem cell biology. Development *139*, 4297–4310. https://doi.org/10.1242/dev.080515.

106. Syed, M.H., Mark, B., and Doe, C.Q. (2017). Playing Well with Others: Extrinsic Cues Regulate Neural Progenitor Temporal Identity to Generate Neuronal Diversity. Trends Genet. TIG *33*, 933–942. https://doi.org/10.1016/j.tig.2017.08.005.

107. Ito, K., and Hotta, Y. (1992). Proliferation pattern of postembryonic neuroblasts in the brain of Drosophila melanogaster. Dev. Biol. *149*, 134–148. https://doi.org/10.1016/0012-1606(92)90270-q.

108. Truman, J.W., and Bate, M. (1988). Spatial and temporal patterns of neurogenesis in the central nervous system of Drosophila melanogaster. Dev. Biol. *125*, 145–157. https://doi.org/10.1016/0012-1606(88)90067-x.

109. Truman, J.W., Schuppe, H., Shepherd, D., and Williams, D.W. (2004). Developmental architecture of adult-specific lineages in the ventral CNS of Drosophila. Development *131*, 5167–5184. https://doi.org/10.1242/dev.01371.

110. Prokop, A., and Technau, G.M. (1991). The origin of postembryonic neuroblasts in the ventral nerve cord of Drosophila melanogaster. Development *111*, 79–88. https://doi.org/10.1242/dev.111.1.79.

111. Truman, J.W., and Riddiford, L.M. (2019). The evolution of insect metamorphosis: a developmental and endocrine view. Philos. Trans. R. Soc. Lond. B Biol. Sci. *374*, 20190070. https://doi.org/10.1098/rstb.2019.0070.

112. Truman, J.W., and Riddiford, L.M. (2023). Drosophila postembryonic nervous system development: a model for the endocrine control of development. Genetics *223*, iyac184. https://doi.org/10.1093/genetics/iyac184.

113. Dumstrei, K., Wang, F., Nassif, C., and Hartenstein, V. (2003). Early development of the Drosophila brain: V. Pattern of postembryonic neuronal lineages expressing DE-cadherin. J. Comp. Neurol. *455*, 451–462. https://doi.org/10.1002/cne.10484.

114. Yaniv, S.P., and Schuldiner, O. (2016). A fly's view of neuronal remodeling. Wiley Interdiscip. Rev. Dev. Biol. *5*, 618–635. https://doi.org/10.1002/wdev.241.

115. Truman, J.W., Price, J., Miyares, R.L., and Lee, T. (2023). Metamorphosis of memory circuits in Drosophila reveals a strategy for evolving a larval brain. eLife *12*, e80594. https://doi.org/10.7554/eLife.80594.

116. Lee, K., and Doe, C.Q. (2021). A locomotor neural circuit persists and functions similarly in larvae and adult Drosophila. eLife *10*, e69767. https://doi.org/10.7554/eLife.69767.

117. Andrade, I.V., Riebli, N., Nguyen, B.-C.M., Omoto, J.J., Cardona, A., and Hartenstein, V. (2019). Developmentally Arrested Precursors of Pontine Neurons Establish an Embryonic Blueprint of the Drosophila Central Complex. Curr. Biol. *29*, 412–425.e3. https://doi.org/10.1016/J.CUB.2018.12.012.

118. Riebli, N., Viktorin, G., and Reichert, H. (2013). Early-born neurons in type II neuroblast lineages establish a larval primordium and integrate into adult circuitry during central complex development in Drosophila. Neural Dev. *8*, 6. https://doi.org/10.1186/1749-8104-8-6.

119. Wong, D.C., Lovick, J.K., Ngo, K.T., Borisuthirattana, W., Omoto, J.J., and Hartenstein, V. (2013). Postembryonic lineages of the Drosophila brain: II. Identification of lineage projection patterns based on MARCM clones. Dev. Biol. *384*, 258–289. https://doi.org/10.1016/J.YDBIO.2013.07.009.

120. Truman, J.W. (2019). The Evolution of Insect Metamorphosis. Curr. Biol. *29*, R1252–R1268. https://doi.org/10.1016/j.cub.2019.10.009.

121. Yamanaka, N., Rewitz, K.F., and O'Connor, M.B. (2013). Ecdysone Control of Developmental Transitions: Lessons from Drosophila Research. Annu. Rev. Entomol. *58*, 497–516. https://doi.org/10.1146/annurev-ento-120811-153608.

122. Thummel, C.S. (2001). Molecular mechanisms of developmental timing in C. elegans and Drosophila. Dev. Cell *1*, 453–465. https://doi.org/10.1016/s1534-5807(01)00060-0.

123. Truman, J.W., Talbot, W.S., Fahrbach, S.E., and Hogness, D.S. (1994). Ecdysone receptor expression in the CNS correlates with stage-specific responses to ecdysteroids during Drosophila and Manduca development. Development *120*, 219–234. https://doi.org/10.1242/dev.120.1.219.

124. Handler, A.M. (1982). Ecdysteroid titers during pupal and adult development in Drosophila melanogaster. Dev. Biol. *93*, 73–82. https://doi.org/10.1016/0012-1606(82)90240-8.

125. Fisher, Y.E., Yang, H.H., Isaacman-Beck, J., Xie, M., Gohl, D.M., and Clandinin, T.R. (2017). FlpStop, a tool for conditional gene control in Drosophila. eLife *6*, e22279. https://doi.org/10.7554/eLife.22279.

126. Isaacman-Beck, J., Paik, K.C., Wienecke, C.F.R., Yang, H.H., Fisher, Y.E., Wang, I.E., Ishida, I.G., Maimon, G., Wilson, R.I., and Clandinin,

T.R. (2020). SPARC enables genetic manipulation of precise proportions of cells. Nat. Neurosci. *23*, 1168–1175. https://doi.org/10.1038/s41593-020-0668-9.

127. Cherbas, L., Hu, X., Zhimulev, I., Belyaeva, E., and Cherbas, P. (2003). EcR isoforms in Drosophila: testing tissue-specific requirements by targeted blockade and rescue. Development *130*, 271–284. https://doi.org/10.1242/dev.00205.
128. Hamid, A., Gattuso, H., Caglar, A.N., Pillai, M., Steele, T., Gonzalez, A., Nagel, K., and Syed, M.H. (2024). The conserved RNA-binding protein Imp is required for the specification and function of olfactory navigation circuitry in Drosophila. Curr. Biol. *34*, 473–488.e6. https://doi.org/10.1016/j.cub.2023.12.020.
129. McGuire, S.E., Mao, Z., and Davis, R.L. (2004). Spatiotemporal Gene Expression Targeting with the TARGET and Gene-Switch Systems in Drosophila. Sci. STKE *2004*, pl6. https://doi.org/10.1126/stke.2202004pl6.
130. Wiggin, T.D., Goodwin, P.R., Donelson, N.C., Liu, C., Trinh, K., Sanyal, S., and Griffith, L.C. (2020). Covert sleep-related biological processes are revealed by probabilistic analysis in Drosophila. Proc. Natl. Acad. Sci. USA *117*, 10024–10034. https://doi.org/10.1073/pnas.1917573117.
131. Xu, X., Yang, W., Tian, B., Sui, X., Chi, W., Rao, Y., and Tang, C. (2021). Quantitative investigation reveals distinct phases in Drosophila sleep. Commun. Biol. *4*, 364. https://doi.org/10.1038/s42003-021-01883-y.
132. Hendricks, J.C., Finn, S.M., Panckeri, K.A., Chavkin, J., Williams, J.A., Sehgal, A., and Pack, A.I. (2000). Rest in drosophila is a sleep-like state. Neuron *25*, 129–138. https://doi.org/10.1016/S0896-6273(00)80877-6.
133. van Alphen, B., Yap, M.H.W., Kirszenblat, L., Kottler, B., and van Swinderen, B. (2013). A Dynamic Deep Sleep Stage in Drosophila. J. Neurosci. *33*, 6917–6927. https://doi.org/10.1523/JNEUROSCI.0061-13.2013.
134. Chowdhury, B., Abhilash, L., Ortega, A., Liu, S., and Shafer, O. (2023). Homeostatic control of deep sleep and molecular correlates of sleep pressure in Drosophila. eLife *12*, e91355. https://doi.org/10.7554/eLife.91355.
135. Niki, A., A.l., T.-H.L., Hang, L., Eleni, N., Qiongyi, Z., Trent, P., Philip, B., J., S.P., et al. (2023). Experimentally induced active and quiet sleep engage non-overlapping transcriptomes in Drosophila. eLife *12*, RP88198. https://doi.org/10.7554/eLife.88198.
136. Abhilash, L., and Shafer, O.T. (2024). A two-process model of Drosophila sleep reveals an inter-dependence between circadian clock speed and the rate of sleep pressure decay. Sleep *47*, zsad277. https://doi.org/10.1093/sleep/zsad277.
137. Jain, S., Lin, Y., Kurmangaliyev, Y.Z., Valdes-Aleman, J., LoCascio, S.A., Mirshahidi, P., Parrington, B., and Zipursky, S.L. (2022). A global timing mechanism regulates cell-type-specific wiring programmes. Nature *603*, 112–118. https://doi.org/10.1038/s41586-022-04418-5.
138. Sakamura, S., Hsu, F.-Y., Tsujita, A., Abubaker, M.B., Chiang, A.-S., and Matsuno, K. (2023). Ecdysone signaling determines lateral polarity and remodels neurites to form Drosophila's left-right brain asymmetry. Cell Rep. *42*, 112337. https://doi.org/10.1016/j.celrep.2023.112337.
139. Kohwi, M., Lupton, J.R., Lai, S.-L., Miller, M.R., and Doe, C.Q. (2013). Developmentally regulated subnuclear genome reorganization restricts neural progenitor competence in Drosophila. Cell *152*, 97–108. https://doi.org/10.1016/j.cell.2012.11.049.
140. Xie, X., Tabuchi, M., Corver, A., Duan, G., Wu, M.N., and Kolodkin, A.L. (2019). Semaphorin 2b Regulates Sleep-Circuit Formation in the Drosophila Central Brain. Neuron *104*, 322–337.e14. https://doi.org/10.1016/j.neuron.2019.07.019.
141. Pahl, M.C., Doyle, S.E., and Siegrist, S.E. (2019). E93 Integrates Neuroblast Intrinsic State with Developmental Time to Terminate MB Neurogenesis via Autophagy. Curr. Biol. *29*, 750–762.e3. https://doi.org/10.1016/J.CUB.2019.01.039.
142. Lam, G., Nam, H.-J., Velentzas, P.D., Baehrecke, E.H., and Thummel, C.S. (2022). Drosophila E93 promotes adult development and suppresses larval responses to ecdysone during metamorphosis. Dev. Biol. *481*, 104–115. https://doi.org/10.1016/j.ydbio.2021.10.001.
143. Mou, X., Duncan, D.M., Baehrecke, E.H., and Duncan, I. (2012). Control of target gene specificity during metamorphosis by the steroid response gene E93. Proc. Natl. Acad. Sci. USA *109*, 2949–2954. https://doi.org/10.1073/pnas.1117559109.
144. Ureña, E., Manjón, C., Franch-Marro, X., and Martín, D. (2014). Transcription factor E93 specifies adult metamorphosis in hemimetabolous and holometabolous insects. Proc. Natl. Acad. Sci. USA *111*, 7024–7029. https://doi.org/10.1073/pnas.1401478111.
145. Hobert, O. (2021). Homeobox genes and the specification of neuronal identity. Nat. Rev. Neurosci. *22*, 627–636. https://doi.org/10.1038/s41583-021-00497-x.
146. Sun, H., and Hobert, O. (2023). Temporal transitions in the postembryonic nervous system of the nematode Caenorhabditis elegans: Recent insights and open questions. Semin. Cell Dev. Biol. *142*, 67–80. https://doi.org/10.1016/j.semcdb.2022.05.029.
147. Sun, H., and Hobert, O. (2021). Temporal transitions in the post-mitotic nervous system of Caenorhabditis elegans. Nature *600*, 93–99. https://doi.org/10.1038/s41586-021-04071-4.
148. Özel, M.N., Gibbs, C.S., Holguera, I., Soliman, M., Bonneau, R., and Desplan, C. (2022). Coordinated control of neuronal differentiation and wiring by sustained transcription factors. Science *378*, eadd1884. https://doi.org/10.1126/science.add1884.
149. Fernandez-Nicolas, A., Machaj, G., Ventos-Alfonso, A., Pagone, V., Minemura, T., Ohde, T., Daimon, T., Ylla, G., and Belles, X. (2023). Reduction of embryonic E93 expression as a hypothetical driver of the evolution of insect metamorphosis. Proc. Natl. Acad. Sci. USA *120*, e2216640120. https://doi.org/10.1073/pnas.2216640120.
150. Ishimoto, H., and Kitamoto, T. (2010). The Steroid Molting Hormone Ecdysone Regulates Sleep in Adult Drosophila melanogaster. Genetics *185*, 269–281. https://doi.org/10.1534/genetics.110.114587.
151. Ishimoto, H., Lark, A.R.S., and Kitamoto, T. (2012). Factors that Differentially Affect Daytime and Nighttime Sleep in Drosophila melanogaster. Front. Neurol. *3*, 24. https://doi.org/10.3389/fneur.2012.00024.
152. Li, Y., Haynes, P., Zhang, S.L., Yue, Z., and Sehgal, A. (2023). Ecdysone acts through cortex glia to regulate sleep in Drosophila. eLife *12*, e81723. https://doi.org/10.7554/eLife.81723.
153. Powsner, L. (1935). The Effects of Temperature on the Durations of the Developmental Stages of Drosophila melanogaster. Physiol. Zool. *8*, 474–520. https://doi.org/10.1086/physzool.8.4.30151263.
154. Perrotta, A.T., and Been, M.D. (1991). A pseudoknot-like structure required for efficient self-cleavage of hepatitis delta virus RNA. Nature *350*, 434–436. https://doi.org/10.1038/350434a0.
155. Nagarkar-Jaiswal, S., Lee, P.-T., Campbell, M.E., Chen, K., Anguiano-Zarate, S., Gutierrez, M.C., Busby, T., Lin, W.-W., He, Y., Schulze, K.L., et al. (2015). A library of MiMICs allows tagging of genes and reversible, spatial and temporal knockdown of proteins in Drosophila. eLife *4*, e05338. https://doi.org/10.7554/eLife.05338.
156. Geissmann, Q., Garcia Rodriguez, L.G., Beckwith, E.J., and Gilestro, G.F. (2019). Rethomics: An R framework to analyse high-throughput behavioural data. PLoS One *14*, e0209331. https://doi.org/10.1371/journal.pone.0209331.

STAR★METHODS

KEY RESOURCES TABLE

REAGENT or RESOURCE	SOURCE	IDENTIFIER
Antibodies		
nc82 (anti-Bruchpilot) anti-Mouse	DSHB	Cat# AB_2314866; RRID: AB_2314866
Monoclonal Anti-GFP Chicken	Aves Labs	Cat# GFP-1010; RRID: AB_2307313
Anti-mCherry Polyclonal Rabbit	Novus Biologicals	Cat# NBP2-25157; RRID: AB_2753204
Monoclonal Anti-Dpn Rat	Abcam	Cat# 11D1BC7; RRID: AB_2687586
Anti-Asense Rabbit	Cheng-Yu Lee	N/A
Anti-E93 Guinea Pig	Chris Doe	N/A
Anti-EcR-B1 Mouse	Carl Thummel	N/A
Alexa Flour 647 Anti-Mouse	Jackson ImmunoResearch	Cat# 715-605-151; RRID: AB_2340863
Alexa Flour 647 Anti-Rabbit	Jackson ImmunoResearch	Cat# 711-605-152; RRID: AB_2492288
Alexa Flour 488 Anti-Chicken	Jackson ImmunoResearch	Cat# 703-545-155; RRID: AB_2340375
Alexa Flour 555 Anti-Rabbit	Invitrogen	Cat# A-21429; RRID: AB_2535850
Alexa Flour 555 Anti-Rat	Invitrogen	Cat# A-21434; RRID: AB 2535855
Dylight 405 Anti-Guinea Pig	Jackson ImmunoResearch	Cat# 706-475-148; RRID: AB_2340470
Normal Donkey Serum	Jackson ImmunoResearch	Cat# 017-000-121; RRID: AB_2337258
Normal Goat Serum	Jackson ImmunoResearch	Cat# 005-000-121; RRID: AB_2336990
Chemicals, peptides, and recombinant proteins		
16% Paraformaldehyde	Electron Microscopy Sciences	Cat# 15710
Triton X-100	Sigma-Aldrich	Cat# T8787
Apple Juice	S. Martinelli & Co	N/A
Schneider's Insect medium	Sigma-Aldrich	Cat# S0146
Agar	Sigma-Aldrich	Cat# A1296
DPX mounting medium	Sigma-Aldrich	Cat# 06522
Sucrose	Research products International	Cat# 57-50-1
Xylene	Fisher Scientific	Cat# 1330-20-7, 100-41-4
Experimental models: Strains of Drosophila melanogaster		
23E10-LexA on II	BDSC	RRID: BDSC_52693
23E10-GAL4 on III	BDSC	RRID: BDSC_49032
Pointed-GAL4 on III	Yuh-Nung Jan	N/A
UAS-Dicer (on X Chromosome)	BDSC	RRID: BDSC_58756
UAS-E93RNAi on II	BDSC	RRID: BDSC_57868
UAS-E93RNAi on II	VDRC	DRCE93
UAS-E93HA III	Fly ORF	F000587
LexAopmCD8GFP on III	BDSC	RRID: BDSC_32207
UAS-KKRNAi on II	VDRC	60103
Worniu-GAL4, Ase-GAL80 on II	Chris Doe	N/A
UAS-FLPPEST on X	BDSC	RRID: BDSC_24644
UAS-mCherryRNAi on III	BDSC	RRID: BDSC_35785
Sco/Cyo; TubGAL80^{ts}	BDSC	RRID: BDSC_7018
LexAopFRTstopFRTGFP on III	BDSC	RRID: BDSC_57588
W^{1118}	BDSC	RRID: BDSC_5905
Hs-ATG>KOT>FLP, dpn>FRT-stop-FRT>Cre:PEST; actin^LoxP-GAL80-stopLoxP^LexAP65, LexAop-rCD2RFP-p10-spacer-UAS-mCD8GFP-p10; stg14-KD	Tzumin Lee Lab	N/A

(*Continued on next page*)

Continued

REAGENT or RESOURCE	SOURCE	IDENTIFIER
23E10-LexA; Pointed-GAL4, LexAop-mCD8GFP	This Study	N/A
UAS-Dicer; UAS-E93RNAi	This study	N/A
UAS-Dicer; UAS-KKRNAi	This study	N/A
UAS-E93RNAi; TubGAL80^{ts}	This study	N/A
UAS-FLPPEST; Wor-GAL4, Ase- GAL80; LexAop-FRTstopFRT-mcD8GFP	This study	N/A
UAS-FLP, ActinFRTstopFRTGAL4; EcRFLPStop2.0/ Cyo	This study	N/A
EcRFLPStop2.0/ Cyo	This Study	N/A
UAS-E93-HA	Fly ORF	F000587
UAS-EcR-DN	BDSC	RRID: BDSC_6872
UAS-EcR-B1	BDSC	RRID: BDSC_6469
23E10LexA; 17A12-GAL4, LexAop-MryGFP	This study	N/A
UAS-FLP, ActinFRTstopFRTGAL4; EcRFLPStop2.0/ Cyo; UAS-E93HA/Tm3Sb	This Study	N/A
23E10-GAL4, UAS-mCD8GFP	This Study	N/A
UAS-FLPPEST; Worniu-GAL4, Ase-GAL80; ActinFRTstopFRTGAL4	Chris Doe	N/A
UAS-FLPPEST; EcR-FLPStop2.0/Cyo; UAS-E93-HA/Tm3Sb	This Study	N/A
Software and algorithms		
ImageJ	Fiji	Version: 2.9.0/1.53t
Adobe Photoshop (v24.1.1)	Adobe Systems	https://www.adobe.com/products/photoshop.html
Adobe Illustrator (v27.2)	Adobe Systems	https://www.adobe.com/products/illustrator.html
GraphPad Prism 9	GraphPad Software	https://www.graphpad.com/
R Studio	–	https://www.rstudio.com
Other	–	N/A
Drosophila Activity Monitoring system	Trikinetics	Single-beam DAM system, DAM5H multibeam system

Fly Genotypes with Associated Figures

Experimental line	Main	Supplementary
Wor-GAL4, Ase-GAL80; UAS- FLP PEST; LexAop-FRTstopFRT-mCD8GFP crossed to 23E10-LexA	Figure 1C	N/A
hs-ATG>KOT>FLP, dpn>FRT-stop-FRT>Cre:PEST; actin^LoxP-GAL80-stopLoxP^LexAP65, lexAop-rCD2RFP-p10-spacer-UAS-mCD8GFP-p10; stg14-KD crossed to 23E10-GAL4	Figures 2C–2G	N/A
23E10-LexA/Cyo; Pointed-GAL4, LexAop-mCD8GFP /MKRS To EcRFLPStop2.0/Cyo	Figures 3C, 3C′, 3F, and 3F′	Figures S1F and S1G
23E10-LexA/Cyo; Pointed-GAL4, LexAopm-CD8GFP /MKRS To UAS-FLP, ActinFRTstopFRTGAL4; EcR FLPStop2.0/ Cyo	Figures 3D, 3D′, 3G, and 3G′	Figures S1F′ and S1G’
23E10-LexA/Cyo; Pointed-GAL4, LexAop-mCD8GFP/ MKRS To UAS-EcR-DN	Figures 3E, 3E′, 3H, and 3H′	N/A
Pointed-GAL4 To EcRFLPStop2.0/Cyo	N/A	Figures S1A and S1A′
Pointed-GAL4 To UAS-FLP, ActinFRTstopFRTGAl4; EcR FLPStop2.0/ Cyo	N/A	Figures S1B and S1B′
23E10-LexA; Pointed-GAL4, LexAop-mCD8GFP	N/A	Figures S1C and S1C′

(*Continued on next page*)

Continued

Experimental line	Main	Supplementary
23E10-LexA; Pointed-GAL4, LexAop-mCD8GFP To UAS-EcRB1	N/A	Figures S1D and S1D′
23E10-GAL4, UAS-mCD8GFP	Figures 4A–4A″	N/A
23E10LexA/Cyo; Pointed-GAL4, LexAop-mCD8GFP/MKRS To UAS-Dicer; UAS-KKRNAi/Cyo	Figures 4B, 4B′, 4F, and 4F′	Figures S3A–S3A″; Figures S4A and S4A′
23E10-LexA/Cyo; Pointed-GAL4, LexAop-mCD8GFP/MKRS To UAS-Dicer; UAS-E93RNAi/Cyo	Figures 4C and 4C′	Figures S3B–S3B″; Figures S4B and S4B′
23E10-LexA/Cyo; Pointed-GAL4,LexAop-mCD8GFP/MKRS To UAS-E93-HA	Figures 4D and 4D′	Figures S3C–S3C″
23E10-LexA/Cyo; Pointed-GAL4,LexAop-mCD8GFP/MKRS To UAS-FLP, ActinFRTstopFRTGAL4; EcR FLPStop2.0/ Cyo: UAS-E93-HA/Tm3Sb	Figures 4E, 4E′, 4G, and 4G′	Figures S3D–S3D″
UAS-Dicer; Pointed-GAL4 To UAS-KKRNAi	N/A	Figure S2A
UAS-Dicer; Pointed-GAL4 To UAS-E93RNAi	N/A	Figure S2B
23E10-LexA/Cyo; Pointed- GAL4, LexAop-mCD8GFP/MKRS To UAS-mCherryRNAi	N/A	Figures S2C and S2C′
23E10-LexA/Cyo; Pointed- GAL4, LexAop-mCD8GFP/MKRS To UAS-E93RNAi (BDSC)	N/A	Figures S2D and S2D′
23E10-LexA/Cyo; Pointed- GAL4, LexAop-mCD8GFP/MKRS To UAS-FLPPEST; EcR-FLPStop2.0/Cyo; UAS-E93-HA/Tm3Sb	N/A	Figures S2E and S2E′; Figures S3E–S3E″
UAS-FLPPEST; Worniu-GAL4, Ase-GAL80; ActinFRTstopFRTGAL4 To UAS-E93-HA	N/A	Figures S3F–S3F″
23E10-LexA/Cyo; 17A12-GAL4, LexAop-MyrGFP/MKRS To UAS-Dicer; UAS-KKRNAi/Cyo	Figures 5A, 5A′, 5D, and 5D′	N/A
23E10-LexA/Cyo; 17A12-GAL4, LexAop-MyrGFP/MKRS To UAS-Dicer; UAS-E93RNAi/Cyo	Figures 5B, 5B′, 5E, and 5E′	N/A
23E10-LexA/Cyo; 17A12-GAL4, LexAop-MyrGFP/MKRS To UAS-FLP, ActinFRTstopFRTGAL4; EcR FLPStop2.0/ Cyo	Figures 5C, 5C′, 5F, and 5F′	N/A
23E10-LexA/Cyo; Pointed-GAL4, LexAop-mCD8GFP/MKRS To UAS-E93RNAi (VDRC RNAi line without dicer)	Figures 6C and 6C′	N/A
23E10-LexA/Cyo; Pointed-GAL4, LexAop-mCD8GFP/MKRS To UAS-E93RNAi; TubGAL80ts	Figures 6D–6F′	N/A
W1118 to UAS-E93RNAi	Figure 7	N/A
Pointed-GAL4 to UAS-KKRNAi	Figure 7	N/A
Pointed-GAL4 to UAS-E93RNAi	Figure 7	N/A

EXPERIMENTAL MODEL AND SUBJECT DETAILS

All flies (Drosophila melanogaster) were maintained on conventional Bloomington Food formulation at ~25C, ~65% relative humidity, and under a 12-hour light/dark cycle (lights on at 7 AM) throughout development and adulthood unless otherwise stated. The egg-laying for RNAi and FLPStop experiments was performed at 25C, and then hatched larvae were transferred and allowed to develop at 29C until adult stages. Also, standardized age matching conversions were used for GAL80ts experiments: 18C is 2.25X slower than 25C, and 29C is 1.03X faster than 25C.[153] The genotype information of the flies used in each experiment is listed in the key resources table.

To knock down E93 in NSCs, we initially used E93 RNAi (from the VDRC stock center) along with UAS Dicer, and the phenotype we observed was severe. Later, we used the same E93 RNAi without dicer, and a similar phenotype was observed. We also used a second independent E93 RNAi line from BDSC stock center, which gave a similar phenotype.

METHOD DETAILS

Immunostaining

Brains from L3 larvae or 5–7 day old adult flies were dissected in ice-cold insect media (Schneiders media) (Sigma Aldrich) and fixed in 4% paraformaldehyde (PFA) (EMS) in PBST (1X phosphate-buffered saline with 0.5 % Triton X-100) for 27 min at room temperature. Following fixing, three 20-minute washes in 1X PBST were performed, and brains were blocked for 40 minutes in blocking solution PBST containing 2.5% Normal Goat serum and 2.5% Normal Donkey Serum (Jackson ImmunoResearch) at room temperature. After blocking, brain samples were incubated with primary antibody at 4C overnight for larvae and two nights for adult brains. Brains were rinsed and washed thrice for 20 minutes in PBST and then incubated with secondary antibody for 2 hours at room temperature for larvae brains and for adult brains for two nights 4C. After the secondary antibody, brains were rinsed again, and three 20-min PBST washes were performed. After antibody staining, DPX mounting was performed on brain samples. For DPX mounting, the protocol from Janelia FlyLight was followed.

The dilutions for various primary antibodies are as Chicken anti-GFP (1:1500), Rat anti-Dpn (1:500), Rabbit anti-Asense (1:500), Mouse anti- Bruchpilot (nc82) (1:50), Mouse anti-EcR-B1 (1:2000), Rabbit anti-mCherry (1:500), Guinea Pig anti-E93 (1:300).

Microscopy

Fluorescent image stacks of whole-mount fly brains were taken using Zeiss LSM 710 and 780 confocal microscopes. In the final paper figures, only slices corresponding to the FB neuropil (stained with nc82) were shown, giving an exact idea about the axonal targeting of dFB neurons in CX. For 23E10 dFB neurons stained with GFP, the slices that give the full projection of these neurons were shown. Image stacks were processed with Fiji (ImageJ), and Adobe Photoshop. Figures were composed using Adobe Illustrator.

Clonal analysis and birthdating

The CLIn fly females, and cell class-specific males were allowed to mate in a bottle and then shifted to an egg-laying cage. The egg laying was done on apple agar caps. The eggs were allowed to hatch at 25C. Then, newly hatched larvae 0-3.5hr old were manually collected and reared on food caps (at 25C) until the desired time point. For lineage mapping of cell class-specific neurons, larvae were heat shocked at 37C at Zero ALH. The zero ALH heat shock (for lineage determination) duration was determined and customized to get a single NSC clone one time. The most effective heat shock time was 10-12 minutes at 37C to get individual NSC clones. The individual NSC clones obtained were compared to an already available source.[64] For temporal birth dating the neurons from a particular cell class lineage, the 50-minute heat shock was performed at 0h, 48h, and 76h ALH. The larvae were transferred to undergo normal development at 25C and dissected as adults. Both male and female adult flies were dissected in our experiments.

Generation of FLPStop2.0 plasmid for transgenesis

The original FLPStop1.0 was generated to allow for conditional gene control in *Drosophila*.[125] For some genes, for unknown reasons, the FLPStop1.0 cassette did not abrogate expression of the transcript in the presence of FLP Recombinase, though the authors speculated about potential readthrough of transcriptional and translational stop sequences.[125] The FLPStop2.0 cassette was updated to include a 10x repeated sequence of the self-cleaving ribozyme from the Hepatitis Delta Virus (HDV)[154] (Figure 3A). In other molecular constructs, this sequence has been shown to effectively disrupt transcription and expression of transgenes.[126]

The pFLPStop2.0-attB-UAS-2.1-tdTom plasmid was generated through the synthesis of the FLPStop 2.0 cassette (Figure 3A) and molecular cloning into the FLPStop-attB-UAS-2.1-tdTom[125] by Genscript (Piscataway, NJ, USA). Constructs were sequence-verified by single primer extension (Sequetech; Mountain View, CA) and were submitted to Addgene. Transgenic flies harboring the FLPStop 2.0 cassette generated through injection of the plasmid and insertion within an intron of EcR, as described below.

Generation of FLPStop2.0 transgenic flies

Transgenic flies harboring the FLPStop 2.0 cassette in an intron of EcR were generated via standard construct injection (~50ng plasmid) by Bestgene (Chino Hills, CA, USA). The MiMIC strain[155] used for injection was y[1] w[*]; Mi{y[+mDint2]=MIC}EcR [MI05320] (Bloomington Drosophila Stock Center Stock 38619). Four transgenic lines were identified through the loss of *y* and were PCR-tested for orientation of insertion by Bestgene. We then tested these lines for expression of TdTomato and gene disruption after conditional expression of FLP Recombinase (Figures S1A–S1B′). The transgenic line for conditional disruption of EcR was isolated and has been maintained.

Sleep assays

Sleep behavior was measured using the Drosophila Activity Monitoring (DAM) system (Trikinetics, Waltham MA). Single-beam DAM2 monitors were used for sleep deprivation experiments, and multi-beam DAM5H monitors were used for all other sleep experiments. Newly eclosed male flies from crosses were collected and aged in group housing on standard food. Flies were then anesthetized on CO2 pads and loaded into glass tubes (70mm x 5mm x 3mm) containing 5% sucrose and 2% agar medium. Juvenile adult flies were loaded at ~ZT6 on the day of eclosion; mature adult flies were loaded at the same time but after aging for 6-8 days. To deprive flies of sleep, mechanical shaking stimulus was applied by attaching DAM2 monitors to microplate adapters on vortexers (VWR). Monitors were shaken for 2 seconds randomly within every 20-second window for 12 hours during ZT12 – ZT24. Activity counts were collected

every minute, and periods of inactivity lasting at least 5 minutes were classified as sleep; for long sleep bout analysis, only inactivity lasting at least 60 minutes was counted. Sleep parameters were analyzed with a custom R script using Rethomics package.[156]

QUANTIFICATION AND STATISTICAL ANALYSIS

For all figures, excluding Figure 7, the numbers of adult brain cell bodies were manually counted using the Fiji cell counter plug-in. Graphs were created using GraphPad Prism. All experimental P values are the result of one-way ANOVA or Student's test provided by GraphPad Prism unless otherwise stated. The one-way ANOVA was followed by Dunnett's Test or Šidák's Multiple Comparison Test. Error bars are represented as mean ±SD. Asterisks indicate levels of significant differences (*: $p<0.05$, **: $p<0.01$, ***: $p<0.001$, ****: $p<0.0001$, NS, non-significant).

For Figure 7, statistical analysis was performed using GraphPad Prism. Error bars represent SEM; *: $p<0.05$, **: $p<0.01$, ***: $p<0.001$, ****: $p<0.0001$, NS, non-significant by Kruskal-Wallis test with Dunn's multiple comparison corrections.

The sample sizes are denoted in the figure legend.

Current Biology, Volume *34*

Supplemental Information

Stem cell-specific ecdysone signaling regulates the development of dorsal fan-shaped body neurons and sleep homeostasis

Adil R. Wani, Budhaditya Chowdhury, Jenny Luong, Gonzalo Morales Chaya, Krishna Patel, Jesse Isaacman-Beck, Matthew S. Kayser, and Mubarak Hussain Syed

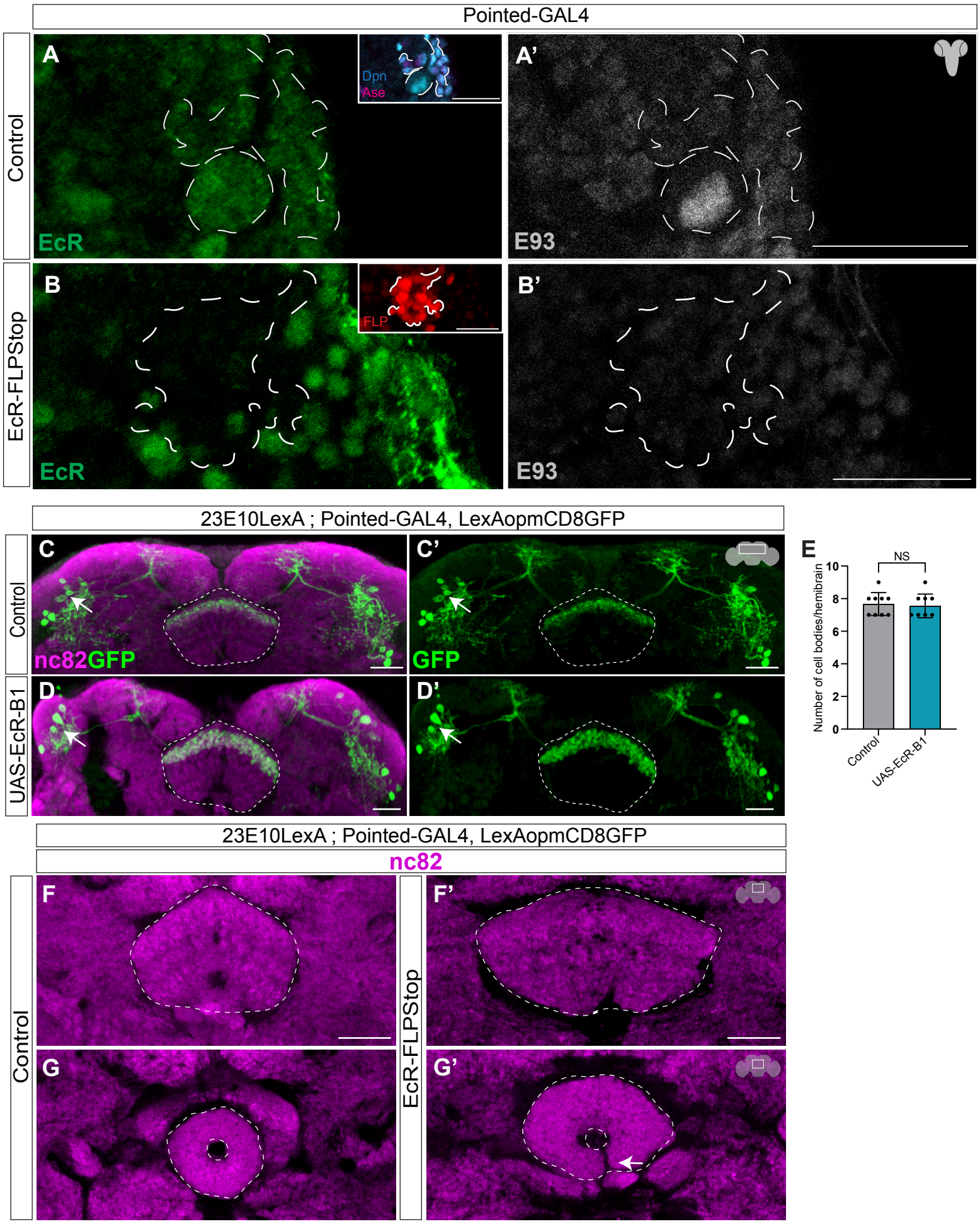
Pointed-GAL4
Control
EcR-FLPStop
A
Dpn
Ase
EcR
A'
E93
B
FLP
EcR
B'
E93
23E10LexA ; Pointed-GAL4, LexAopmCD8GFP
Control
UAS-EcR-B1
C
nc82GFP
C'
GFP
D
D'
E
NS
Number of cell bodies/hemibrain
10
8
6
4
2
0
Control
UAS-EcR-B1
23E10LexA ; Pointed-GAL4, LexAopmCD8GFP
nc82
Control
EcR-FLPStop
F
F'
G
G'

Figure S1. EcR expression in Type II NSCs is necessary for proper central complex development. Related to Figure 3

A-B') EcR-FLPStop is sufficient to reduce EcR expression in Type II NSCs

A, A') EcR and E93 are expressed in L3 larval Type II NSC lineages (outlined). NSCs are identified by Dpn+ Ase-expression (see inset).
B, B') EcR-FLPStop triggered by FLP expression in Pointed-GAL4 pattern leads to a loss of EcR and E93 in L3 larval Type II NSCs. The inset (red color) shows the FLP-based disruption happening in the Type II lineages.
Scale bars represent 20μm. n= 14 larval brains.

C-E) EcR is not sufficient to generate ectopic 23E10 dFB neurons
C, C') 23E10 dFB neurons labeled by a GFP reporter in control brains.
D, D') 23E10 dFB neurons labeled by GFP upon EcR-B1 overexpression in Type II NSCs showing no change in cell body number or morphology.
E) Quantification of the number of 23E10 dFB cell bodies per hemibrain.
Error bars represent ±SD. Asterisks indicate the level of statistical significance: *p<0.05, **p<0.01, ***p<0.001, **** p<0.0001, NS, non-significant by Student t-test.
Cell bodies are indicated by white arrows. The dashed line outlines the FB..

Scale bars represent 20μm. n= 9 adult hemibrains for each genotype.

F-G') EcR is required for normal EB development
F, G) The morphology of the neuropil structures, FB, and EB in control brains.
F', G') Type II NSC-specific EcR loss of function results in defective morphology of the EB while the FB is normal.
Scale bars represent 20μm. n= 12 adult hemibrains for each genotype.
nc-82 labels the neuropil structures. Dashed lines outline FB and EB.

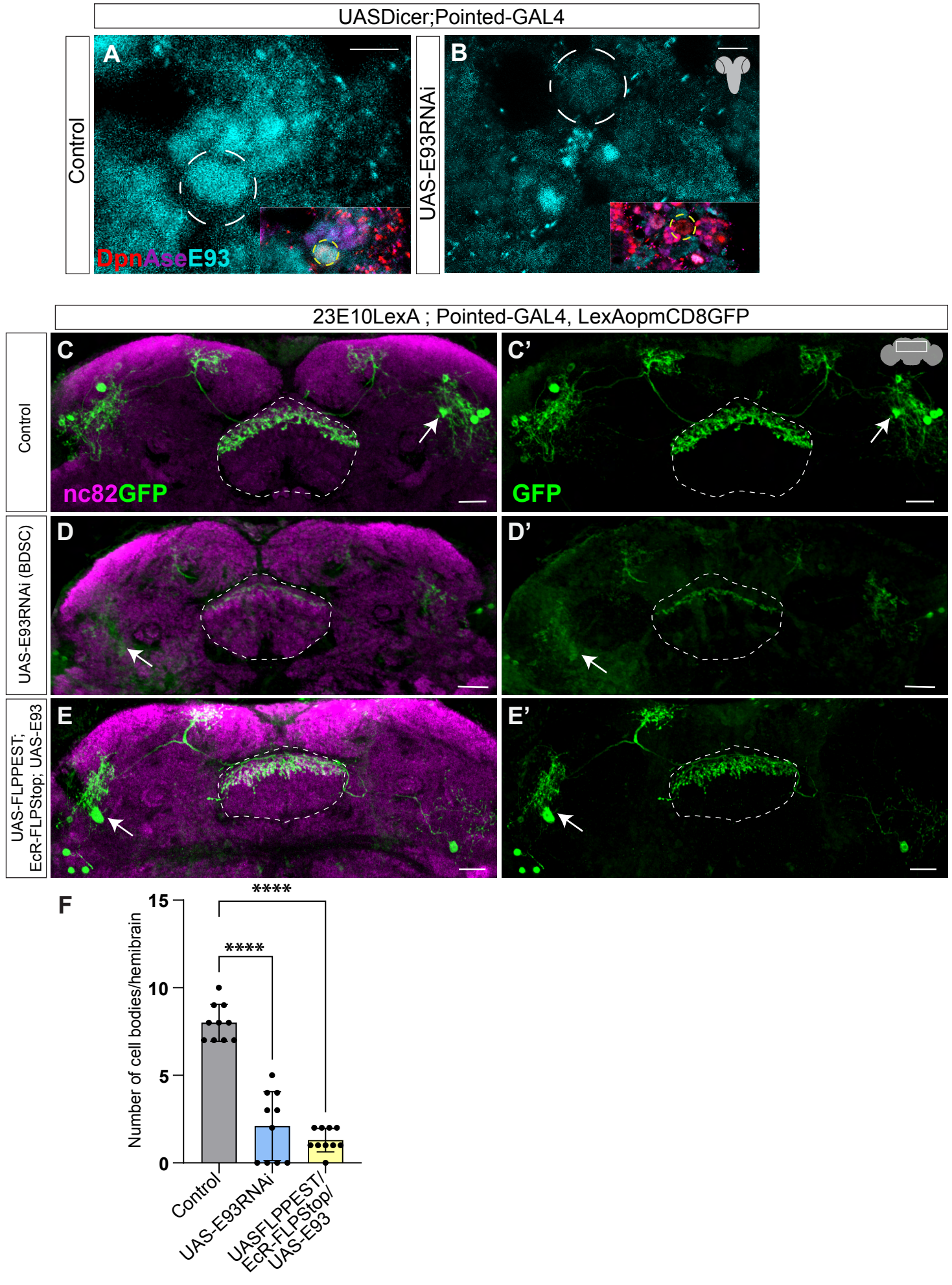
UASDicer;Pointed-GAL4
Control
A
DpnAseE93
UAS-E93RNAi
B
23E10LexA ; Pointed-GAL4, LexAopmCD8GFP
Control
C
nc82GFP
C'
GFP
UAS-E93RNAi (BDSC)
D
D'
UAS-FLPPEST; EcR-FLPStop; UAS-E93
E
E'
F
Number of cell bodies/hemibrain
15
10
5
0
****
****
Control
UAS-E93RNAi
UASFLPPEST/ EcR-FLPStop/ UAS-E93

Figure S2. E93 is necessary but not sufficient for 23E10 dFB neuronal fate. Related to Figure 4

A-B) E93 RNAi expression in Type II NSCs knocks down protein expression effectively

A) Shows expression of E93 in Type II NSCs.
B) Significant loss of E93 in Type II NSCs upon E93 RNAi expression. Small panels in both brains depict the Dpn and Ase staining, which are used to locate the Type II NSCs. Scale bars represent 5μm. n= 4 adult larval brains.

C-E) E93 phenotype is specific to E93 knockdown, and it alone cannot rescue the 23E10 dFB phenotype

C, C') 23E10 dFB neurons expressing reporter GFP in control.
D, D') 23E10 dFB neurons are not specified in E93 RNAi (Pointed-GAL4>E93RNAi BDSC) adult flies.
E, E') Expression of UAS-E93 under Pointed-GAL4 fails to rescue 23E10 dFB neurons in EcR loss of function background (E, E').

F) One-way ANOVA test (followed by Dunnett's Multiple Comparison Test) quantification of 23E10 dFB neurons cell bodies per hemibrain.
Error bars represent ±SD; Asterisks indicate the level of statistical significance:
*p<0.05, **p<0.01, ***p<0.001, **** p<0.0001, NS, non-significant.
Cell bodies are indicated by white arrows. Dashed line outlines the FB.

Scale bars represent 20μm. n= 10 adult hemibrains for each genotype.

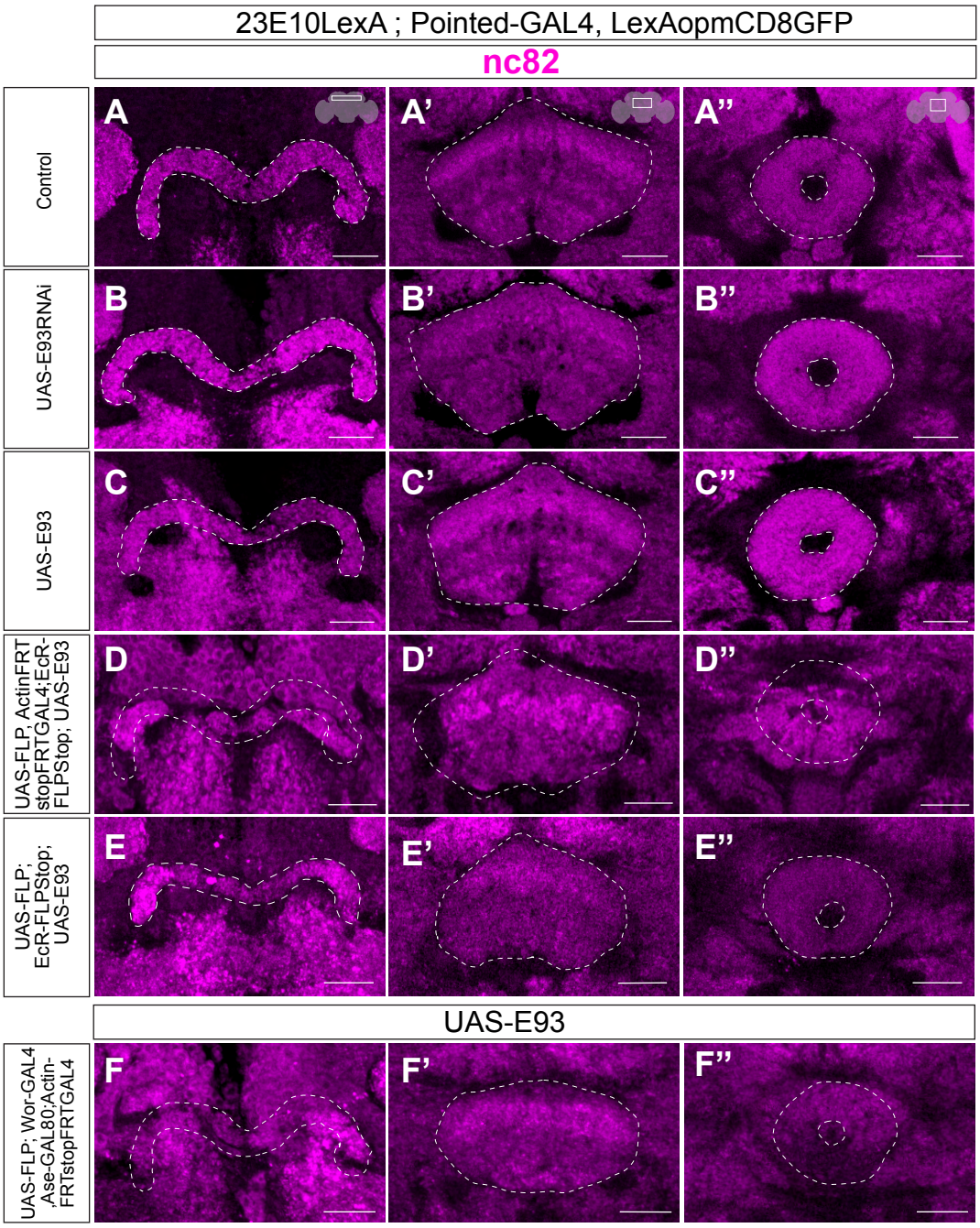
23E10LexA ; Pointed-GAL4, LexAopmCD8GFP
nc82
Control
UAS-E93RNAi
UAS-E93
UAS-FLP; ActinFRT stopFRTGAL4;EcR-FLPStop; UAS-E93
UAS-FLP; EcR-FLPStop; UAS-E93
UAS-E93
UAS-FLP; Wor-GAL4 ,Ase-GAL80;Actin-FRTstopFRTGAL4
A
A'
A''
B
B'
B''
C
C'
C''
D
D'
D''
E
E'
E''
F
F'
F''

Figure S3. Precise E93 expression levels in Type II NSC lineages are critical for proper central complex development. Related to Figure 4

A-F'') Role of E93 in CX neuropil morphology

A-A'') The morphology of three CX neuropil structures, PB, FB, and EB, in control flies.
B-C'') The CX neuropil morphology remains unchanged in E93 RNAi and overexpression flies.
D-D'') Defective CX morphology upon ectopic E93 expression in Type II NSCs using Pointed-GAL4 with lineage tracing cassette of Actin-GAL4 in EcR loss of function background.
E-E'') Without lineage tracing cassette of Actin-GAL4, the CX neuropil morphology remains unaffected upon E93 over expression in EcR loss of function background.,
F-F'') misexpression of E93 in all Type II NSC derived lineages results in abnormal CX neuropil morphology.

nc82 labels the neuropil of adult fly brain.
Dashed lines outline the PB, FB and EB.

Scale bars represent 20μm. n= 5 adult hemibrains for each genotype.

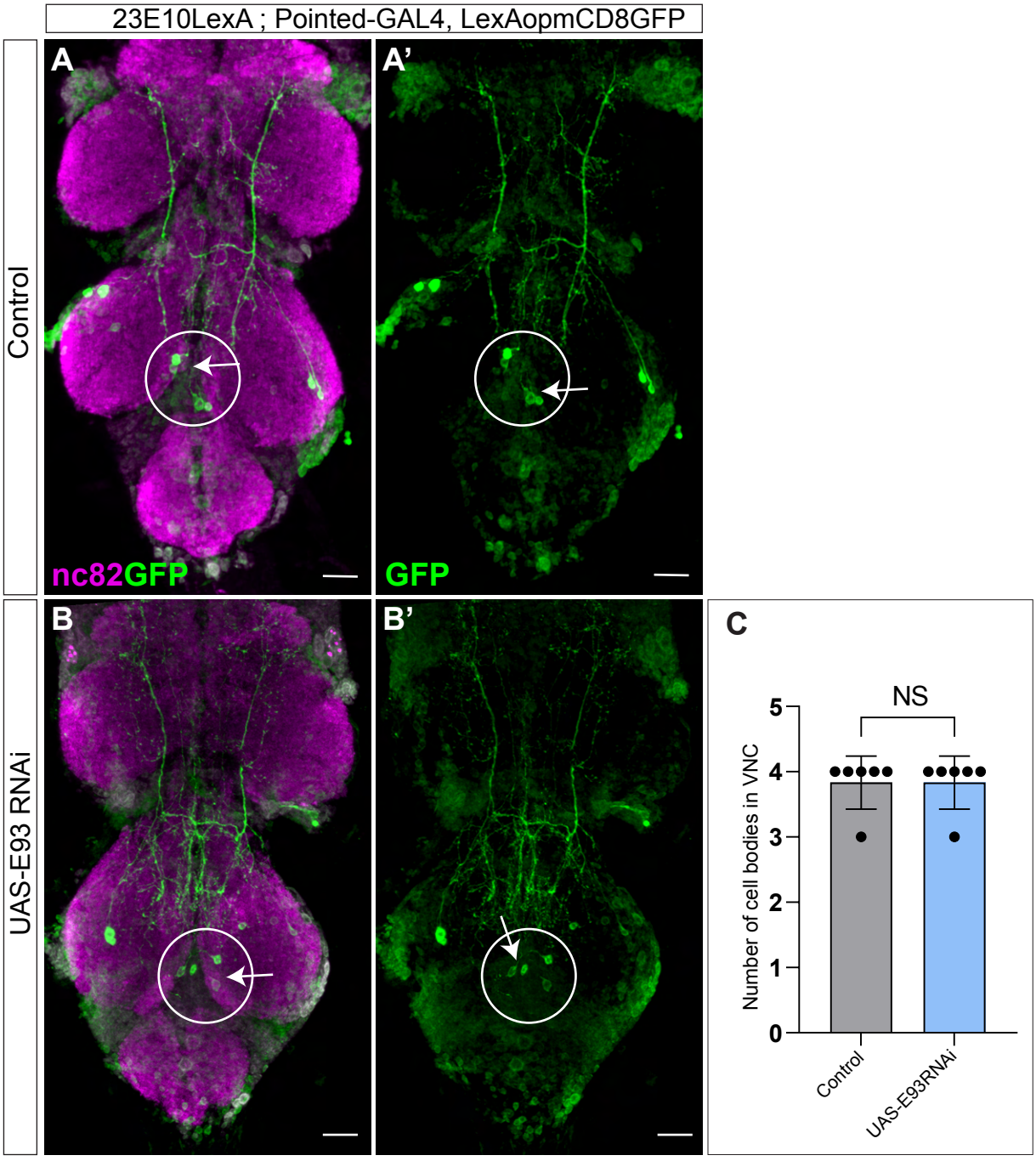
23E10LexA ; Pointed-GAL4, LexAopmCD8GFP
Control
UAS-E93 RNAi
A
A'
B
B'
nc82GFP
GFP
C
NS
Number of cell bodies in VNC
0
1
2
3
4
5
Control
UAS-E93RNAi

Figure S4. E93 knockdown in Type II NSCs selectively affects brain 23E10 labeled neurons but not those in the ventral nerve cord (VNC). Related to figure 7

A, B') shows cell bodies of 23E10+ VNC neurons in control flies.
B, B) no change in the 23E10+ VNC cell body numbers upon E93 knockdown.
C) Quantification of the number of cell bodies per VNC in control and RNAi flies.
Error bars represent ±SD; Asterisks indicate the level of statistical significance:
*p<0.05, **p<0.01, ***p<0.001, **** p<0.0001, NS, non-significant by Students t-test.
Cell bodies indicated by white arrows.

Scale bars represent 20μm. n= 6 adult brain VNCs for each genotype.